RECOMBINATION LIFETIME ANALYSIS
OF DEEP LEVELS IN SILICON.

by

Murray John Robinson

Dissertation submitted to the faculty of the

Virginia Polytechnic Institute and State University

in partial fulfillment of the requirements for the degree of

DOCTOR OF PHILOSOPHY

in

Physics

APPROVED:

T.E.Gilmer Jr.,chairman

--------------------	--------------------
C.D.Williams	A.L.Ritter
--------------------	--------------------
T.E.Leinhardt	J.R.Ficenec

July, 1984

Blacksburg,Virginia

Acknowledgements

Foremost I gratefully acknowledge the assistance and support of my advisor Professor Tom Gilmer.

Many others supplied advice and assistance which was invaluable; principally Professors Ritter, Leinhardt, Williams, and Bowen, as well as the personnel of the Physics machine shop and electronics shop.

The impurity doped samples were kindly donated by JPL and Westinghouse Labs.

Finally, and not least, I gratefully acknowledge the help and support of my wife Marian.

TABLE OF CONTENTS.

I.	Introduction	1
II.	Recombination Centers	6
III.	Defect Structures in Silicon.	14
IV.	The Hall, Shockley, Read Theory.	20
(i)	Derivation of the HSR equations.	20
(ii)	Experimental uses of the HSR equations.	26
V.	Experimental Procedure.	30
(i)	Experimental setup.	31
(ii)	Corrections and limitations.	34
(iii)	Sample preparation.	38
(iv)	Heat treatments.	39
(v)	Impurities.	41
VI.	Results.	45
VII.	Discussion.	70
Conclusion.		84
References.		85
Vita.		88

I. INTRODUCTION

For a semiconductor at thermal equilibrium there is a time averaged number of charge carriers available which is a function of the host material, the temperature and the amount and type of impurities added. There is a thermal generation rate of carriers exactly balanced by a recombination rate. By injection of a non-equilibrium carrier density and observing the return to equilibrium it is possible to derive information concerning the mechanism of recombination.

There are three main classes of recombination mechanisms, direct recombination, impurity/defect recombination and surface recombination.(ref.1)

The third mechanism, surface recombination, occurs due to the lack of periodicity at a surface. This gives a different set of localized levels from the bulk. Clearly all experimental techniques have to consider the effect of these levels on a measurement. Further discussion of this will be left to Section III.

Direct recombination is the mechanism one would expect from a perfect crystal, where the electron and hole recombine directly across the gap, releasing a photon with energy E(gap). In a direct gap semiconductor where the minimum energy gap occurs at zero momentum, direct recombination is the major mechanism for carrier

recombination. This makes these materials useful for applications such as solid state lasers where a precise energy photon is required. Direct recombination is well understood both theoretically and experimentally.

However, for an indirect gap such as silicon and germanium, the minimum energy gap requires the emission or absorption of a phonon to conserve crystal momentum in order to have a direct recombination of a carrier pair. This makes this process far less likely. For example, calculations of excess carrier lifetimes for silicon and germanium due to direct recombination show that these lifetimes are the order of seconds.Experimentally such lifetime measurements usually give less than a millisecond, therefore it can be assumed that another recombination mechanism is dominating.

This third mechanism is the least understood and is recombination via a defect or impurity center.(refs.1,11,13) The recombination occurs in several stages,first a charge carrier (say an electron) is captured at the center which lies deep in the energy gap. The center system then has two choices. It can either reemit the electron back to the conduction band in which case the center is known as a trap, or it can then capture a hole from the valence band and then allow the electron and hole to recombine , leaving the center free to repeat the cycle. The properties of the recombination centers are parametrized in terms of their

capture cross sections for holes(σ_p) and electrons(σ_n) and their energy levels (R).

Certain properties of recombination centers can be intuitively deduced. Efficient recombination centers must be able to capture both holes and electrons, therefore, σ_n and σ_p must be of a similar magnitude. Also to avoid reemission of a captured carrier the centers energy level needs to be away from the conduction or valence bands and towards the middle of the gap. However, it is also found that the charge of the center, although important, is not always decisive. In some cases(Ni,Au centers in Ge) the σ_n of a negative center can exceed σ_n of a neutral center. Clearly the magnitudes of the cross sections depend on the chemical nature and physical structure of the center, but also it is found that the cross sections can be a function of the electric field strengths involved in their measurement.(refs.11,13)

Also of primary interest is the temperature dependence of the cross sections; if this can be determined it can indicate the mechanism by which the energy of recombination is dissipated. This will be discussed further in the next section.

To date there are no unassailable sets of parameters (σ_n,σ_p,R) assigned to a specified recombination center in silicon, which is the most studied material. The main

reasons for this are the complex nature of the centers, their low density, and difficulties in the interpretation of experimental data in terms of these parameters.

Theoretical calculations have at best a tenuous link to experimental observations. The reasons for this are fundamental to the problem. For shallow donor/acceptor states the impurity can be described by an effective mass, hydrogenic theory.As the binding energy is small the state is delocalized and the host material can be described by an effective dielectric constant. However, as the state moves deeper into the gap the atomic-like nature of the host becomes more important as the state becomes more localized. Electron-lattice distortion and defect structure becomes as important as the long-range defect potential. This makes the parameters difficult to calculate.

Theoretical techniques have been applied from two opposite viewpoints.(ref.6) The cluster model builds up the host material incorporating a specific defect structure. The energy levels and other parameters can then be calculated using wavefunctions for the individual atoms in the cluster. The perturbational approach starts off with a set of perfect crystal host wavefunctions and incorporates the defect as a perturbing potential. Both approaches have their shortcomings. The latter approach has the problem of choosing a set of host wavefunctions which converge rapidly

enough to make calculations practical. The cluster methods suffer from the problem of not being able to reduce the influence of the surfaces with practical cluster sizes. Also even large clusters of hostlike atoms do not reproduce the known silicon band structure accurately enough without some sort of muffin tin approach, which is unrealistic in a defect center calculation. Neither approach includes electron-lattice interaction satisfactorily. At present the perturbation techniques seem to offer the best hope for the immediate future.(ref.6)

In this dissertation an experimental method is developed to characterize recombination centers by a technique which uses the recombination lifetime directly. The technique is then used to parametrize recombination centers in silicon introduced by heat treatments and irradiation,and also centers associated with intentionally added impurities.

A high resolution scanning electron microscope is used on selected samples to look for signs of precipitation, and any signs of correlation of precipitation with electrical properties is evaluated.

II.RECOMBINATION CENTERS

As was indicated in the previous section, a recombination center can be parametrized in terms of a single localized energy level within the band gap and capture cross sections for positive and negative charge carriers. By using these parameters it may be possible to deduce more fundamental properties of the center such as its structure and the mechanisms by which the energy of recombination is dissipated. In this section a comparison of the experimental techniques is made, and possible energy dissipation processes are introduced.

II.i Experimental measurements (refs.6,12)

All measurements in studies of recombination centers involve transitions between the localized energy levels and the continuum bands. These transitions involve either absorption or emission of energy, usually in the form of photons and/or phonons. Thus absorption or emission of energy appears to be a convenient way to classify the experimental techniques.

First consider absorption; there are two practical methods of injecting the energy needed to excite carriers between levels, phonons(heat) and photons. Thermally stimulated conductivity has been successfully used for measuring activation energies of shallow donor/acceptor

levels and also for deep lying levels in insulators. However,the deep levels in semiconductors occur with extremely low densities. Therefore to see effects due to these levels high resistivity materials must be used. In general these are difficult to obtain and they also limit the scope of the experiment.

Nevertheless, one very important branch of experiments are used which utilize a pn junction to generate a region free of carriers, enabling the excited carriers from the deep levels to be observed. There are many variations of the junction technique. The most recent (deep level transient spectroscopy) gives a spectrum of the energy levels within the gap and is widely used.

Unfortunately there are two fundamental drawbacks to junction experiments. In the presence of a pn junction there are necessarily high electric fields. The effect of high electric fields on recombination centers has been shown to be considerable in many cases (ref.1) and their interaction is not well understood and clearly adds an extra complication to confuse matters. Secondly, the formation of a pn junction requires several heat treatments. These heat treatments themselves may introduce large numbers of recombination centers,which further confuses definitive identification of intentionally introduced centers.

Optical excitation/absorption of shallow donor/acceptor

excited states has been used with considerable success; however,frequency scanning looking for midgap absorptions is complicated by secondary processes such as photothermal excitation of defect states and thermal broadening. The opposite of optical absorption, luminescence,falls into the second category of experimental techniques, observations of emitted energy, in this case photons. Luminescence, like absorption works well for the shallow states and occasionally for deep levels,particularly in direct gap compound semiconductors such as GaAs.

Similar problems exist with luminescence as in absorption studies, such as thermal broadening due to the strong electron-lattice coupling. Also, in indirect gap materials, band to localized level transitions are not very efficient. Nevertheless, luminescence techniques can be very powerful especially for direct gap semiconductors.

The technique developed in this dissertation uses photons to excite excess carriers across the band gap, and uses the decay time to equilibrium to derive the parameters of the recombination centers involved. It has the advantages that it is simple to implement and the levels observed are those of direct technological interest, since many device applications are mainly concerned with carrier lifetimes directly.

The decay rate is related to the recombination center

using a phenomenological model known as the Hall, Shockley, Read(HSR) model. No assumptions are made concerning decay mechanisms or the structure of the center. These should be at least partially reflected in the parameters obtained. The problem of relating the capture cross sections and energy levels experimentally derived to the fundamental physical properties of the centers is discussed below.

II.ii.Decay Mechanisms (refs.1,6,7,11)

The magnitude and temperature dependence of the capture cross sections are directly connected with the decay mechanism between two energy levels. This dependence can be discussed easily in the context of a configuration coordinate diagram (figure 1). Each parabola represents a single electronic state and the horizontal lines represent lattice vibrational states. This diagram assumes that the electronic and vibrational states are independent of each other (Condon approximation).

Clearly the optical absorption transition AB is not the same as the transition CD, also the minimum energy AC is not the same as the total energy measured by a luminescence or absorption experiment. This gives an idea of the complexities of optical experiments in the presence of a strong electron-lattice interaction.

The capture cross section is directly proportional to the squared modulus of the matrix element connecting the two

states. However, in the presence of strong electron-lattice coupling, a non-radiative transition can occur, which as the name implies involves emission/absorption of phonons only. Pictorially this can be visualized as a vibrational excitation of state 2 (fig.1) to the point E, then de-excitation by the cascading emission of phonons to the point A. However, this is somewhat misleading and can produce large errors in capture cross section calculations. This occurs due to the breakdown of the Condon approximation as the lattice-relaxation coordinate increases.

The breakdown can best be described by the electron-lattice interaction increasing the mixing Hamiltonian between the two states, until(at a point analogous to E) it becomes energetically favorable to decay, by phonon emission, down a path like EA. Thus state 2 has become state 1 without photon emission. Using this mixing correction in the cross section calculation gives non-radiative decay parameters of a similar magnitude to radiative decay values. The temperature dependence of the cross sections offers the best method of determination which process is dominant for a particular recombination center. The exact form of the capture cross sections is dependent on the initial and final states of the transition. Theoretically these states are highly model and potential dependent, thus exact calculations of cross sections have limited value. However,

temperature dependences under certain limiting conditions have been predicted.(refs.1,11)

Since the usual energy of transition to a deep level is greater than the Debye temperature times Boltzmann's constant, non-radiative transitions require a multiphonon mechanism. For temperatures less than the Debye temperature and for a center which has a weak phonon coupling, say a neutral point defect which causes little lattice distortion, the capture cross section is proportional to $e^{-E/kT}$. Where E is an activation energy equivalent to E_E-E_C in figure 1.

The emission of several phonons at once has a relatively small probability of occurring. Far more probable is the cascade process predicted by Lax(ref.1). This model requires a long range potential which allows the defect to have many excited states with a small energy difference between them, say I. Now the captured carrier can cascade through these levels releasing phonons at each step. The temperature dependence of cross section in this case is dependent on the relative magnitudes of I,kT_D and kT. Typically the temperature dependence is T^{-n} (n=2.5 to 4), where n depends on the type of phonon emitted.

For an attractive coulombic potential the cascade process is thought to be the dominant mechanism, although for high equilibrium carrier concentrations screening effects have to be considered. Screening lengths for samples

used in this study are at least several hundred angstroms.

Passler(ref.17) considers attractive, neutral and repulsive centers and gives their temperature dependencies for temperatures less than the Debye temperature as follows:

$$\sigma^{attr}=C/T$$

$$\sigma^{neutr}=C/T^{1/2}$$

$$\sigma^{rep}=CT^{-7/6}e^{-KT^{-1/3}}$$

He notes that for the repulsive case, due to the uncertainty in C and K the temperature dependence is uncertain. Also for many attractive long range potentials the cascade process may dominate.

Finally, other mechanisms for dissipating the recombination energy have been considered which are thought to be unlikely to occur except in special circumstances. For example, with a high density of carriers and defect centers an Auger process can be visualized where two electrons are captured on the same center(or neighbouring centers), a hole is then able to recombine with one electron by donating its energy to the other electron. Other energy dissipation processes such as other bulk excitations (plasmons, excitons) are always considered unlikely processes.

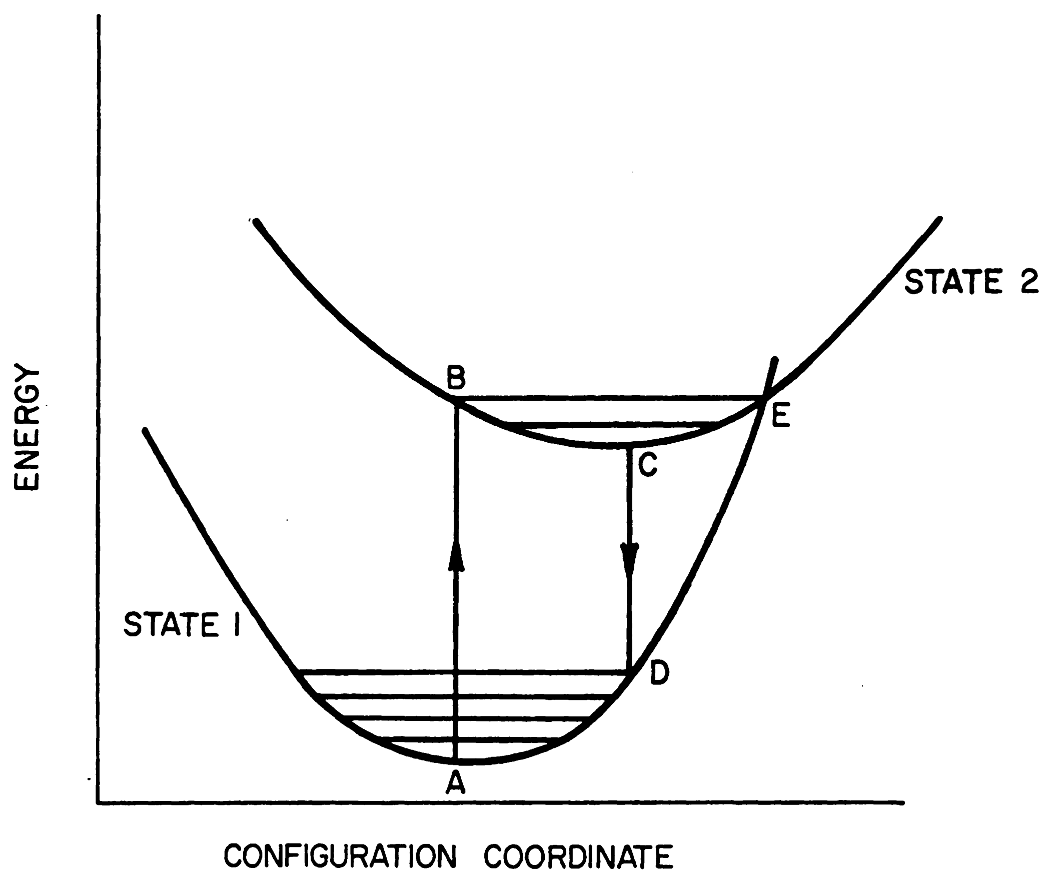

Figure I. CONFIGURATION COORDINATE DIAGRAM SHOWING POSSIBLE ENERGY TRANSITIONS.

III. DEFECT STRUCTURES IN SILICON

The identification of a particular defect structure/type as that belonging to a specific recombination center is probably the most difficult problem in the investigation of deep levels in silicon.(refs.6,8,13) This is partly due to the low densities involved, which makes experimental identification difficult, but also to the large number of possible defects and the interdependency of impurities and structural defects in even the most purified silicon.

Approximately seventy percent of the silicon used in the semiconductor industry is Czochralski (CZ) grown single crystal silicon. This has typical oxygen concentrations of 10^{17} to $10^{18}/cm^3$ and carbon concentrations greater than $10^{16}/cm^3$.

Modern techniques allow silicon to be grown virtually dislocation free, but high magnification under electron microscopes has indicated other classes of structural defects known as microdefects which may form nucleating centers for electrically active impurities. It should also be noted that during the elevated temperatures used for silicon processing, planar defects(stacking faults) may be formed as well as dislocations generated from the stress caused by impurity precipitation. Also present in the formation of silicon devices for silicon studies are

concentrations of metals left over from the silicon purification processes, and significant concentrations of doping materials. Any of these in conjunction with heat treatments may introduce recombination centers. Considering that a titanium or vanadium recombination center density of less than $10^{12}/cm^3$ is enough to degrade solar cell performance, the task of identifying specific centers can be formidable.

The field of defects in silicon is immense and not well understood, though it has been extensively studied and documented. Nevertheless a brief discussion of some of the properties of oxygen in silicon is both relevant to this dissertation and worthwhile for displaying the complexity of defect reactions.

As stated before, oxygen concentrations of 10^{17} to $10^{18}/cm^3$ are typical in CZ silicon. In float zone (FZ) silicon, which uses radio frequency heating rather than a resistively heated silica crucible, oxygen concentrations two orders of magnitude lower can be obtained. However, this is still significant compared with typical dopant concentrations.

Oxygen in as-grown single crystal silicon occupies an interstitial position in the host lattice.(ref.8) It introduces a multiplicity of defect states, but none of these are observable in the forbidden gap in appreciable

quantities. On heat treatments between 300-500C for extended periods of time (several hours), oxygen forms a shallow donor complex thought to be SiO_4. At about 650C, small precipitates of SiO_2 are formed, which when followed by high temperature heat treatments(900-1250C) can act as nucleation centers for dislocations, stacking faults or further precipitation of oxygen or other impurities. Also any oxygen donor complexes previously formed are dissolved after 30 minutes of heat treatment at 650C. Between 700 and 1000C oxygen can precipitate at dislocations and, depending on the carbon content of the silicon, oxygen/carbon complexes can form further donor structures(ref.16).

At temperatures between 1000 and 1250C,which are typically used for diffusion processes, the situation is further confused by the interaction of microdefects and point defects which can diffuse in from surface abrasions.(ref.13) These structural defects are thought to play a critical role by acting as nucleation centers for large scale precipitation of oxygen, as the oxygen becomes more mobile at these temperatures. Above 1300C the oxygen precipitates begin to go back into solution as the melting point of silicon(1410C) is approached and the solubility limit of oxygen in silicon is reached.

Also, it is known that thermal defects (vacancies,interstitials) play a critical role in

recombination center formation. Two major types of these microdefects have been observed. "A" type defects are small dislocation loops often decorated with impurities, and "B" type defects are much smaller and remain uncharacterized. Their mechanisms of formation and interaction are not understood.

Fabrication of a pn junction requires several high temperature heating and cooling steps during which the defect structure may be continually modified. Clearly a technique that can be used to investigate centers produced by a single heat treatment is of considerable interest. It is important to remember that although the defects described have many energy levels associated with them,it is only those that fall within the band gap and that are electrically active as recombination centers that are of interest in this study.

The recombination centers in silicon are highly dependent on the sample purity, heat treatment history and crystallinity. The table following gives a brief summary of the major intrinsic defects documented to date and describes their thermal properties.(refs.3,8,10,13,16)

A particularly puzzling effect that this dissertation attempts to address is the introduction of significant numbers of recombination centers by short time, low temperature heat treatments. The recombination centers

associated with these defects are highly dependent on sample and experimental conditions. Their moderate densities and the sensitivity of carrier lifetimes make them ideal subjects for the technique developed here. Studies of these centers, which provide the nucleating impetus for mass catastophic defect introduction at higher device processing temperatures, have not been possible using standard techniques, and it is hoped this study will help clarify and identify the interactions between structural microdefects and impurities, a topic which is so far poorly understood.

Table 1:Energy levels introduced in silicon through heat treatments.

Recombination center	Heat treatment needed	Energy levels associated	Annealing behaviour
j-center divacancy	slow cool from 650C	E_V+0.25-0.3eV	Anneals at 350C
Si-A center V-O complex	slow cool from 650C	E_C-0.17eV	Anneals at 300-400C
Si-E center V-P complex		E_C-0.4eV	Anneals at 100C
Shallow donor Si-O complex	slow cool from 500C	E_C-(0.08-0.1eV)	dissolves at 650c
vac cluster/ Fe-vacancy	quench	E_V+0.4eV	Both RT and 300C reported
strain/surface diffused def.	1000-1200C heating	E_C-0.254eV E_C-0.54eV	Anneal by 1250-650C slow cool

IV. THE HALL, SHOCKLEY, READ(HSR) THEORY.

IV.i Derivation of the HSR equations. (refs. 4,5,9)

The HSR theory is a simple phenomenological theory relating recombination center parameters(R,σ_n,σ_p) to excess carrier decay time, which is experimentally observed.

List of Symbols

R/C/F:- energy of recombination center/conduction band minimum/fermi level(for simplicity the highest valence band energy is set to zero)

N:- total density of recombination centers

N^0/N^-:- density of unoccupied/occupied recombination centers

σ_n/σ_p:- capture cross sections for electrons/holes

v:- thermal velocity of charge carriers

N_c/N_v:- effective density of states at the conduction/valence band edge

τ_{n0}/τ_{p0}:- carrier lifetime if all the centers are full of holes/ electrons

The theory starts with the following basic premise: rate of capture of carriers = (volume swept out by carrier per second)x(density of recombination centers available for capture)x(density of carriers), (ref.5) e.g.

$$R_n=(v\sigma_n)x(N^0)x(n) \quad (1)$$

Similarly,

$$R_p = v\sigma_p N^- p \quad (2)$$

Using (1) and the definition of lifetime, $\tau = n/(dn/dt)$, gives

$$\tau_{1n} = n/R_n = 1/(v\sigma_n N^0) \quad (3)$$

where τ_{1n}=lifetime of a free electron.

In thermal equilibrium, $R_n^{emission} = R_n^{capture}$, thus

$$R_n^{em} = N^-/\tau_{2n} = n_0/\tau_{1n}$$

where τ_{2n}=lifetime of captured carrier, thus

$$\tau_{2n} = N^-/(v\sigma_n n_0 N^0) \quad (4)$$

In equilibrium, N^-= Nx(probability of center being occupied), thus

$$N^- = N(1/(1+e^{(R-F)/kT})) \quad (5)$$

By conservation of the number of traps at equilibrium,

$N = N^0 + N^-$, thus,

$$N^0 = Ne^{(R-F)/kT}/(1+e^{(R-F)/kT}) \quad (6)$$

In nonequilibrium the following holds for the total rate of recombination of electrons:

$$dn/dt=-n/\tau_{1n}+N^{-}/\tau_{2n}=-v\sigma_{n}(N^{0}n-n_{1}N^{-}) \quad (7)$$

where $n_1=N_c e^{(R-F)/kT}$.

It should be noted that (7) gives the rate of removal of carrier electrons from a unit sample volume due to recombination only. In cases where additional mechanisms of electron removal occur, such as a field effect in junction experiments, the rates for these mechanisms have to be included in (7). Also in cases where constant illumination of the sample is used, an electron generation term has to be added. The photoconductive decay methods have the advantage that the rate equation (7) is reduced to its simplest form.

By making the substitution $n \rightarrow n_0+\delta n$, the rate equations for the decay of excess carriers are obtained.

$$d(\delta n)/dt=-\sigma_{n}vN^{0}\delta n \quad (8)$$

$$d(\delta p)/dt=-\sigma_{p}vN^{-}\delta p \quad (9)$$

Both N^- and N^0 are functions of R, F, n, p, T. These equations can be solved exactly under the constraints of conservation of trap number, electrical charge and small δn, δp.(ref.4)

The solution can be generalized for larger magnitudes of δn, δp(ref.5) subject to the constraints

$$\delta n<N^{0}+n_{0}+n_{1} \quad (10)$$

$$\delta p < N^- + p_0 + p_1 \quad (11)$$

The solution is of the form

$$\delta n = A_n e^{-t/\tau_1} + B_n e^{-t/\tau_2} \quad (12)$$

τ_1 is a time constant which corresponds to the rearrangement time of the excess carriers on the recombination centers. Under the experimental arrangement of this study τ_1 is too short to be measured and τ_2 is the measured lifetime(τ_m) and is given by

$$\tau_m = \tau_0 (1+A)/(1+[n_0 \delta n/(n_0+n_1) + p_0 \delta p/(p_0+p_1)] x X) \quad (13)$$

where

$$\tau_0 = [\tau_{p0}(N^0+n_0+n_1) + \tau_{n0}(N^- + p_0 + p_1)] x X$$

$$A = (\tau_{p0} \delta n + \tau_{n0} \delta p) x X$$

$$X = (n_0 + p_0 + N^- N^0/N)^{-1}$$

As it stands (13) is too unwieldy to use and the following experimental approximations are introduced:

i) Only n-type silicon is used, thus $n_0 >> p_0$.

ii) Noting that $n_0/n_1 = p_1/p_0 = e^{(F-R)/kT}$, and under the constraint that $\tau_m = \tau_2$, $(dN^-/dt=0)$, then

$$N^-/N^0 = (\sigma_n n + \sigma_p p_1)/(\sigma_p p + \sigma_n n_1)$$

Using the assumption that F>R, which is reasonable if the recombination level is deep enough or the material is strongly n-type, then the following simplifications occur(noting kT is small):

$$n_0 >> n_1$$

$$p_1 >> p_0$$

Therefore, $N^- >> N^0$, thus, by conservation of traps, $N^- = N$. Also $N^- N^0 / N = 0$, and $X = 1/n_0$.

Equation (13) is now reduced to:

$$\tau_m = \tau_0 (1 + B/n_0)/(1 + \delta n / n_0) \quad (14)$$

where,

$$\tau_0 = \tau_{p0} + \tau_{n0} N / n_0 + \tau_{n0} p_1 / n_0 \quad (15)$$

$$B = \tau_{p0} \delta n + \tau_{n0} \delta p \quad (16)$$

Clearly, the opposite assumption can be made (F<R) for not so strongly n-type samples. The major requirement is that during the experiment F must never be close to R.

iii) The final assumption required in order to obtain a practical (experimentally usable) equation is that $\delta p = \delta n$. By using the conservation of charge, $\delta n = \delta N^- + \delta p$,then clearly $\delta n = \delta p$ under the conditions $\delta n \approx n_0 >> N$. This corresponds to the situation where the band carriers have to wait for the recombination centers to empty themselves, or $\sigma_n >> \sigma_p$ where the hole density controls the electron density due to the

immediate recombination of a band electron with a captured hole.

These conditions are difficult to recognize experimentally, the first being the only condition which is under experimental control. Clearly, a necessary test for these assumptions is their self-consistency with the experimental results.

Equations (14)-(16) can now be reduced to their final form:

$$\tau_m=\tau_0(1+ax)/(1+x) \quad (17)$$

$$\tau_0=\tau_{p0}+\tau_{n0}N/n_0+\tau_{n0}(N_v/n_0)e^{-R/kT} \quad (18)$$

$$a=(\tau_{n0}+\tau_{p0})/\tau_0 \quad (19)$$

$$x=\delta n/n_0 \quad (20)$$

IV.ii Experimental uses of the HSR equations

Equation (17) is the most commonly quoted form of the HSR theory under conditions of equal rates of recombination for holes and electrons, and the assumptions stated in the previous section. Experimentally these conditions can occur under constant illumination, or pulsed illumination(decay) experiments where τ_2 is the dominant lifetime.

Constant illumination experiments have been used with some success, and they have the advantage that they are simple to implement experimentally.(ref.5) However, the

lifetime has to be derived by calculating the efficiency of photon generation within the sample as a function of the illumination intensity. The generation rate is then given by

$(dn/dt)_{gen}$=gxIntensity, where g=efficiency of photon generation. Then

$$\tau_m = n_{excess}/(dn/dt)_{gen}$$

Clearly the fact that the lifetime is also dependent on the excess density is also unsatifactory.

The major difficulty with pulsed illumination experiments is obtaining an acceptable measurement of the lifetime for large values of $x(\delta n/n_0)$. For small values of x, $\tau_m \rightarrow \tau_0$ and x(t) can be approximated by an exponential decay.However,in order to determine a(eq.(19)), the lifetime has to be measured instantaneously for a set of x. This data is difficult to obtain and subject to biased errors. For this reason excess carrier decay curves have had limited usefulness in recombination center analysis.

However, by expressing (17) as a differential equation and integrating, a more useful form is obtained:

$$\tau_m = \delta n/(d(\delta n)/dt) = x/(dx/dt) = \tau_0(1+ax)/(1+x)$$

which gives upon integration by parts,

$$t=(a-1)\tau_0 \ln[(1+x)/(1+x_0)]+\tau_0 \ln[x/x_0] \quad (21)$$

where x_0=x evaluated at arbitrary t=0.

This equation has the advantage that both x and t can be measured to a reasonable accuracy. Thus a set of x,t fitted to an equation of form (21) will give a(T) and $\tau_0(T)$ as fitted parameters. Unfortunately the pathological form of (21) requires determination of x,t to high accuracies in order to obtain reasonable confidence limits for a and τ_0. This is probably the major reason why (21) has not been mentioned in the literature or used as an experimental basis. However, by using a microcomputer system to improve the accuracy of the x,t measurements and statistically enhance the data fits, the advantages of pulsed illumination experiments are used to develop a simple, non-destructive technique for recombination center analysis.

A typical fit using this technique is shown in figure 2. The Y variable represents lifetime, the X variable is a function of excess density and time as given by equation (21). The Y intercept is τ_0 and the slope $(a-1)\tau_0$. This clearly shows the error introduced by simply assuming an exponential fit at low excess densities.

To summarize: pulsed illumination experiments have several experimental advantages(see next section) over standard techniques used for deep level characterization. However, the errors in the determination of lifetimes have prevented their use in determination of the HSR parameters

for recombination centers. The method developed and used in this study gives a much more accurate lifetime measurement. This permits reproducible, accurate fits to the HSR equations, and makes determination of the HSR parameters possible.

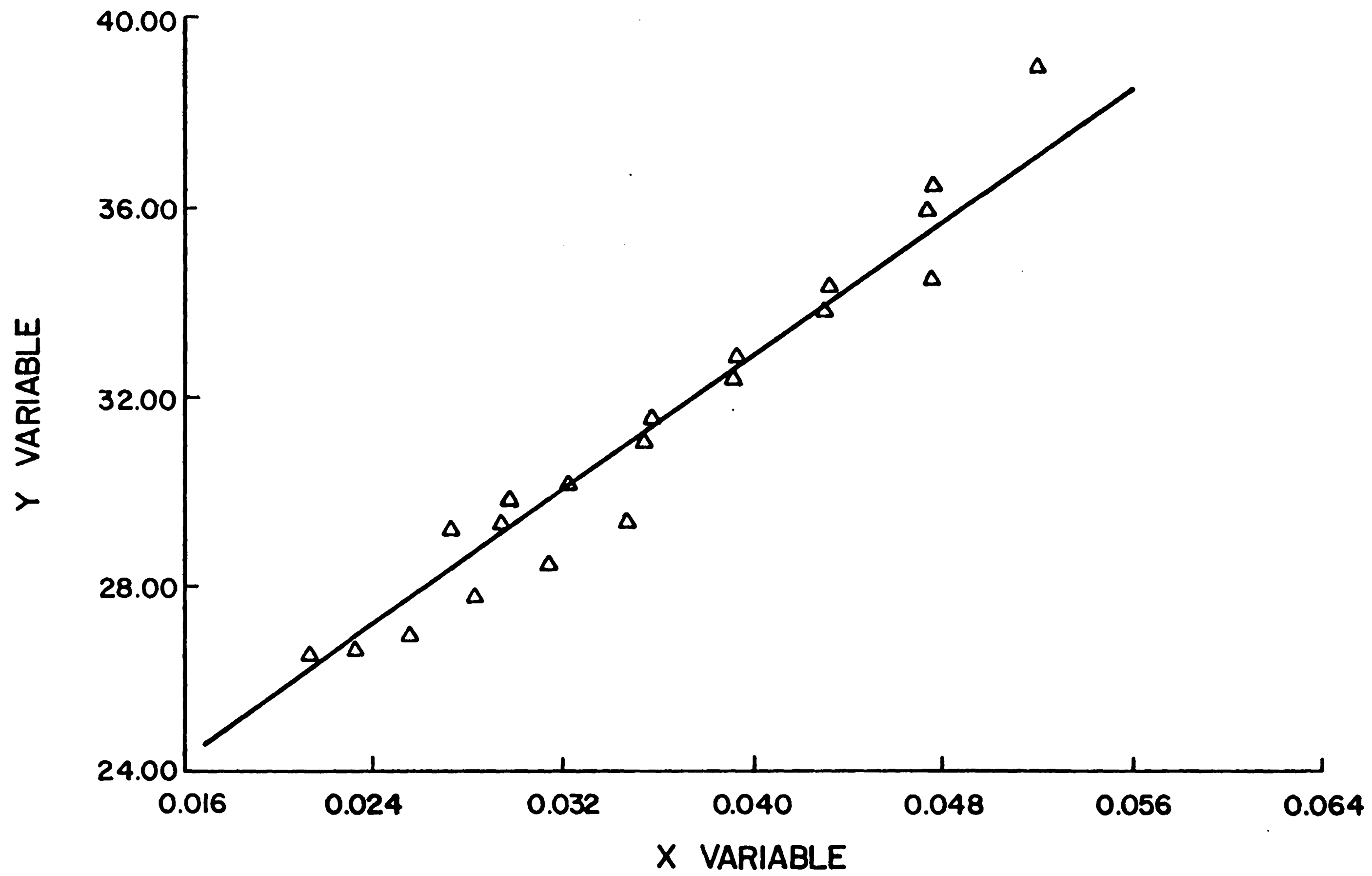

Figure 2. TYPICAL PLOT FOR LIFETIME DATA

V. EXPERIMENTAL PROCEDURE.

List of Symbols

$\delta n/\delta p$:- excess density concentrations of electrons/holes

δV:- change in voltage across sample due to above

μ_e/μ_p:- mobility of electrons/holes

I:- current through sample

V_0:- equilibrium voltage across sample

A:- cross sectional area of sample

l:- sample length illuminated

The experimental procedure is very simple in essence. The silicon sample is illuminated with a pulse of high intensity band-gap light to generate a large number of excess carriers. Then by monitoring the decay of the excess conductivity to equilibrium the required data is obtained.

The conductivity is related to the number of excess carriers by

$$\sigma=n_0 e\mu_e \qquad (1)$$

Noting that since we are using n-type silicon the majority carriers are electrons, and the excess conductivity is given by

$$\delta\sigma=e(\mu_e+\mu_h)\delta n \qquad (2)$$

after using the fact that $\delta p=\delta n$.

The conductivity is simply related to the voltage measurement on the scope by placing a large non-inductive resistance in series with the silicon sample. This ensures that the current flowing through the sample is kept constant at all excess carrier densities(within 2%). Thus by using (2) and $\sigma_0=(I/V)(A/l)$,

$$\delta\sigma=[I/(V_0-\delta V)](A/l)=e(\mu_e+\mu_h)\delta n$$

$$\delta n=\sigma_0[1/(e\mu_e+e\mu_h)]x[1/(1-\delta V/V_0)]$$

$$x=\delta n/n_0=[\mu_e/(\mu_e+\mu_h)]x[1/(1-\delta V/V_0)] \quad (3)$$

Thus $x(t)$ is simply related to the voltage decay measured,and by using standard relationships for the mobilities it is easily calculated.(ref.15)

V.i. Experimental setup

The experimental arrangement is shown schematically in figure 3. The light source used is a commercial xenon arc flashtube. Extra capacitor banks are added and the light is concentrated onto the sample to increase intensity. Directly before the sample is a 2mm thick silicon filter: this reduces the amount of highly absorbed light on the sample so as to ensure a more homogeneous distribution of the excess carriers in the bulk of the sample. The sample

is placed inside two grounded aluminum boxes, and coaxial connecting cables are used throughout to minimize pickup from the high voltage transients used in the light source.

To provide temperature control of the sample the inner aluminum box is heated using electrical heating tape, while the outside box is kept at 273K by ice cooling. Between the two boxes is loosely packed insulation. This combination of heating and cooling enables the rate of temperature change to be closely controlled. The sample is kept in contact with a ceramic block which acts as a heat sink, and the temperature is measured using an iron-constantan thermocouple in direct contact with the sample.

The sample is a filament of silicon measuring approximately 2x0.5x0.5cm. A nine-volt battery is placed in series with the sample and the large resistance, the resistance can be adjusted to give an equilibrium sample voltage reading between 0.1 and 0.7 volts.

Electrical contacts are ultrasonically soldered to the sample ends, and brass pressure screws press onto the contacts to complete the circuit and to keep the sample in position. Indium solder is used for the contacts, as this solder forms an ohmic contact with n-type silicon. However,the circuit is tested by illuminating the sample with no applied voltage to ensure that there is no photovoltaic signal.

The experiment is controlled by a TRS 80 microcomputer system which provides the timing, triggering, data taking and data analysis. The data acquisition is performed by a custom built board, using an ultra fast analog to digital converter to digitize the data and provide a "handshake" to the TRS 80. The fastest data rate obtainable(0.2 MHz) is limited by the A/D converter and the machine language execution time of the TRS 80. This rate proves to be adequate for most decay rates of interest in this study.

The data analysis proceeds as follows. First the data is read into the computer and the corrections described in the next section applied, then the set of data $\{x_i, x_0, t_i\}$, i=1 to 25, is fitted to equation IV.(21). This is done for between 150 and 200 temperatures to obtain another set of data $\{a_j, \tau_{0j}, T_j\}$. Using another fitting procedure this set is fitted to an equation of the form IV.(18):

$$\tau_0=A+Be^{-R/kT} \quad (4)$$

$$A=\tau_{po}+\tau_{no}N/n_0 \quad (5)$$

$$B=\tau_{no}N_v/n_0 \quad (6)$$

The fitting procedure gives A, B and R. A and B are taken to be independent of temperature and are used with the set of values $(a\tau_0)_i (=\tau_{n0}+\tau_{p0})$ to derive information about the center. To facilitate examination and comparison of

this last set of values, they are fitted to a quartic with the variable $(1/K_BT)$.

Clearly, to assume that A and B are independent of temperature is an approximation. However, over the temperature ranges used their temperature dependence is small compared with the exponential term.

The major source of error in the procedure lies in the initial data fit to equation IV.(21). For this reason only fits with linear correlation confidence limits greater than 99% are used, and the data from this fit weighted according to correlation coefficient.

A standard deviation for the energy level R is calculated for each fit.(ref.9) Such a calculation is not possible for the capture cross sections, but an average standard deviation is calculated for $a\tau_0$ over the temperature range.

V.ii.Corrections and limitations (ref.9)

Several secondary effects delimit the usefulness of the excess carrier decay technique. Those effects whose contribution can be calculated, such as the surface diffusion lifetime, are corrected by the microcomputer, whereas mass action and shallow trapping effects limit the range of excess carrier generation. Figure 4 shows the contribution of most of these processes to the decay curve. Figure 4 shows computer simulations of these processes.

i) Initial surface recombination arises from the abundance of energy levels and the large mobility of carriers at a surface. This allows carriers to recombine rapidly, giving a fast initial decay time. To offset this the light is passed through a silicon filter to limit the intensity of photons which are highly absorbed by the sample and produce high densities of surface carriers. Also to combat this effect, the initial measurement of δn is delayed by $20\mu s$.

ii) Another unwelcome contribution from surfaces is associated with the surface diffusion lifetime. Carriers in the bulk diffuse to the surface and recombine, giving a concentration gradient of carriers in the sample, with zero at the surfaces and non-zero elsewhere. Therefore the carrier diffusion equation has to be solved subject to these boundary conditions. This gives a surface diffusion lifetime which is dependent on the sample size and shape. This lifetime can be up to 50% of the bulk lifetime and its effect has to be corrected for by the microcomputer. The effect of the surface diffusion lifetime is minimized by using large bulk samples. Typical diffusion lifetimes for samples in this study are 1-2 milliseconds.

iii) Also on the high excess density portion of the decay, error arises from the finite decay of the light pulse. It can be approximated by an exponential decay with a

lifetime of 1-5 microseconds. This has to be convolved with the sample response. However, calculations have shown that if measurements are delayed by 20 microseconds from the light pulse trigger the convolution effects are minimal(less than 3%).

iv) On the low excess density end of the decay the principal error arises from shallow trapping effects. Trapping occurs due to the presence of shallow energy levels which can trap a carrier for a short length of time and then re-release it to the continuum band, thus seemingly increasing its free lifetime. This effect can be minimized by illuminating the sample with a low intensity dc light source to keep the traps empty. However, it is found that the best solution to this problem is to limit the low excess density range to $x_0=0.01$. This solution also removes a problem of lower system resolution due to the A/D conversion.

v) The effects of mass action limit the temperature range of the experiment. The Law of mass action states that the product of the hole and electron densities is constant for any given temperature. Its effects can best be shown using an example. Assume an n-type, 800 ohm-cm silicon crystal at 300K. For this resistivity $n_0=5x10^{12}/cm^3$ and mass action gives $n_0p_0=10^{20}/cm^6$, thus $p_0=4x10^{-6}xn_0$. The sample is strongly n-type and a conductivity measurement would give

n_0. However , at 390K, $n_0p_0=5x10^{24}/cm^6$, and $p_0=0.2xn_0$. Clearly the sample is becoming intrinsic and the validity of the assumptions made in section IV are questioned. Thus the maximum temperature must be limited to a range where the sample remains extrinsic.

iv) Finally, the excess density is calculated from a voltage measurement , equation (3). Clearly the form of the equation increases the error as $\delta V/V$ approaches unity. For this reason a high excess density limit is imposed at x=0.3 (this also helps (i),(ii),(iii)).

It should also be noted that in this study recombination is assumed to be dominated by only one type of center in each sample. Other studies (ref.4) have attempted to consider the situation where multiple centers contribute. However, their success has been limited and their results inconclusive. Over the range of excess densities measured in this experiment, computer simulations show that the difference between two and one level fits is marginal, and measurable effects do not occur until much higher densities.

In defence of the one level fit it seems reasonable to suggest that since a one level fit is just as good as a two level fit to the available data, the introduction of a greater complexity is not justified. In other words,the data should point strongly to a multiple level fit before being assumed.

V.iii.Sample preparation

Three types of phosphorus doped single crystal silicon were used, all obtained as grown from Monsanto electronic materials. Their resistivity and type are as follows:

i) Czochralski grown with oxygen content between 10^{16}-$10^{17}/cm^3$ and resistivity approximately 80 ohm-cm.

ii) Float zone grown(FZ1) with oxygen content $2x10^{15}$-$2x10^{16}/cm^3$ and resistivity approximately 800 ohm-cm.

iii) Float zone grown(FZ2) with low($<10^{15}/cm^3$) oxygen content and resistivity 9000-12000 ohm-cm.

The samples were cut from the silicon boules using a diamond edge saw with the (111) crystal direction along the length of the filament.

The sample faces were ground on silicon carbide paper to remove any deep saw marks, and then etched in a 3:3:5 mixture of concentrated hydrofloric acid, glacial acetic acid and concentrated nitric acid. This removes all surface impurities and flaws and leaves a clean, highly polished surface. The samples were then washed in acetone and stored in clean quartz bottles before use.

Lifetime measurements on untreated samples agreed well with the calculated surface diffusion lifetimes. All three types of silicon gave untreated bulk lifetimes greater than 10 milliseconds.

V.iv.Heat treatments

Looking back at table 1 there appear to be several critical temperature ranges for defect production. These heat treatment ranges of 1000-1200C, 600-650C and 350-500C, plus the subsequent heat treatments (fast quench, slow quench and annealing), have a significant effect on the dominant recombination center produced. All three ranges were tried on each type of silicon and fast and slow quenches applied.

The heat treatments were carried out by heating the samples in an evacuated quartz tube for periods of time which gave an observable bulk decay time(for excess carriers). The treatment times varied from 24 hours for some slow quench, low temperature treatments to several minutes for high temperature fast quenches.

The slow quench consisted simply of turning off the furnace. The cooling rate was non-linear but never exceeded 100C/hour. For a fast quench the sample was tipped from the hot end of the quartz tube to the cooler end which remained just above room temperature: the sample could then be removed from the tube within 30 seconds, giving typical cooling rates of 500-1000C per minute. Faster cooling methods were tried, such as heating the sample directly and quenching in water. It was found that these were difficult to duplicate and hence gave poor reproducibility and in some

cases caused the samples to shatter.

A possible problem existing at these heat treatment temperatures is bulk contamination by fast diffusing impurities, especially for the long heat treatments. Most impurities are extremely slow diffusers at these temperatures and even for the worst case of contamination could only penetrate the top surface. However, copper and lithium have high solubilities and are fast diffusers. The effect of copper was examined by evaporating a copper film on a test sample and using a 350C heat treatment in attempting to diffuse in a significant amount. No variation in decay time or resistivity was observed, and it was concluded that with careful sample preparation extrinsic copper contamination should not be a problem.

Lithium is a slower diffuser than copper but has a much higher solubility. The lithium diffusion is carried out by placing the samples in an oil/lithium solution at 170C for 20 hours, followed by an acetone wash, then a 350C, 20 hour heat treatment to drive in and homogenize the lithium over the sample bulk. Higher initial diffusion temperatures lead to surface pitting of the silicon and high surface concentrations of lithium which are difficult to drive in and give erroneous resistivity measurements. The lithium concentration was estimated in a high resistivity FZ2 sample by noting the carrier concentration as lithium is a shallow

donor. The concentration was estimated to be greater than $10^{14}/cm^3$.

Overall, in the current experiments bulk contamination is not thought to be a problem because bulk samples were used.

V.v. Impurities

Several attempts were made to diffuse fast diffusing impurities into the silicon used for heat treatments. Clearly temperatures less than 350C had to be used in order to avoid heat treatment centers. Diffusion/solubility data at these temperatures is not available. However, extrapolations of available data indicated that diffusion times of several days would be required. Even these treatments failed to introduce enough recombination centers to have a noticeable effect on the lifetime.

For this reason samples were obtained from Westinghouse with impurities grown into the silicon boule. These samples were doped with both boron and phosphorus. Their resistivities varied from 1.5 ohm-cm to 30 ohm-cm. The impurities added were titanium, vanadium, iron, cobalt, molybdenum, chromium, nickel, manganese and copper.

Most samples showed too short a decay time to be measurable using the present equipment. Also the high equilibrium carrier concentration reduced the 'x'

measurement to unmanageable levels. However, by reducing the filter thickness and reflectivity, enough excess density was generated to obtain measurable results for some samples. The fact that some samples were p type instead of n type changes only the details of the analysis, not the validity.

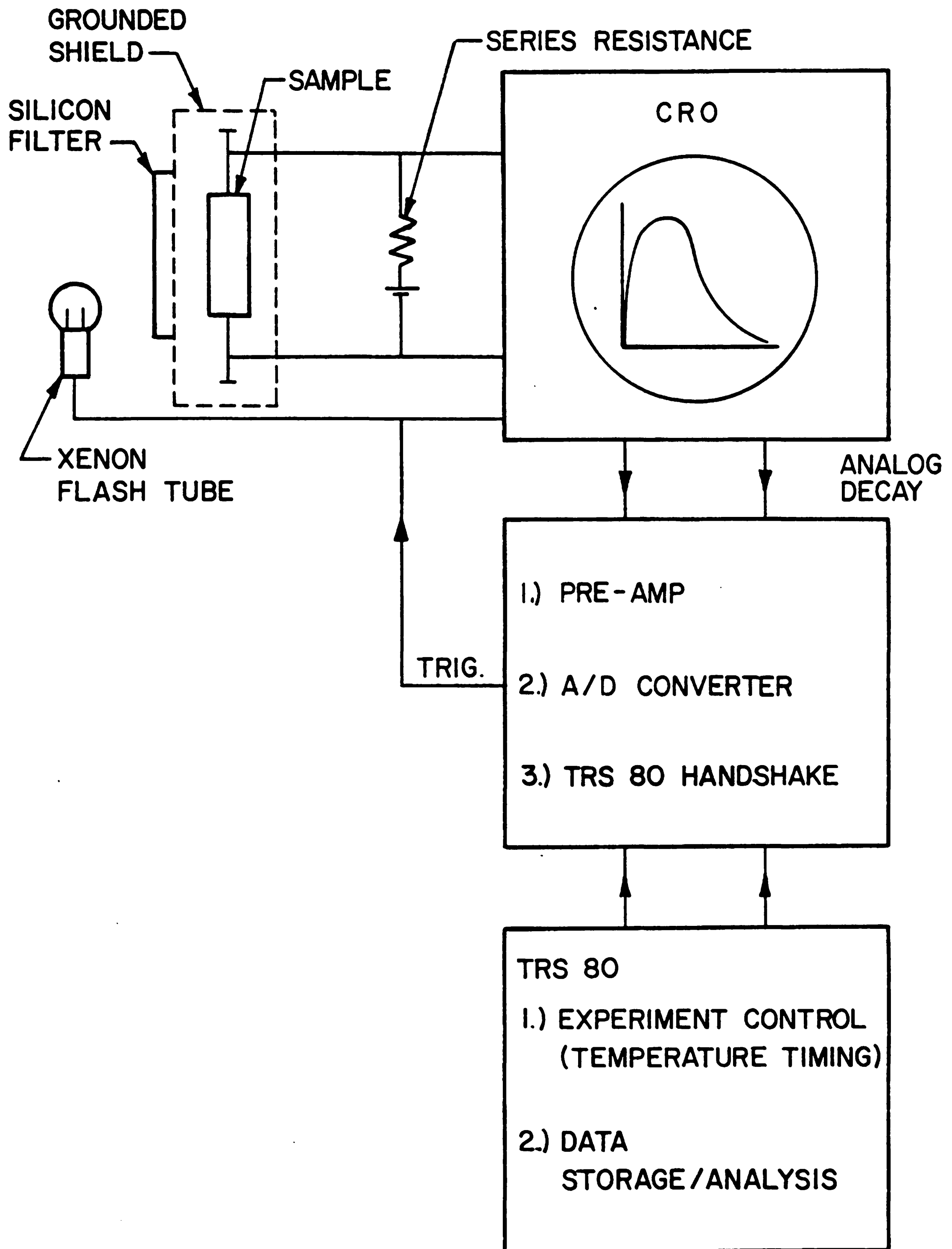

Figure 3. SCHEMATIC EXPERIMENTAL ARRANGEMENT

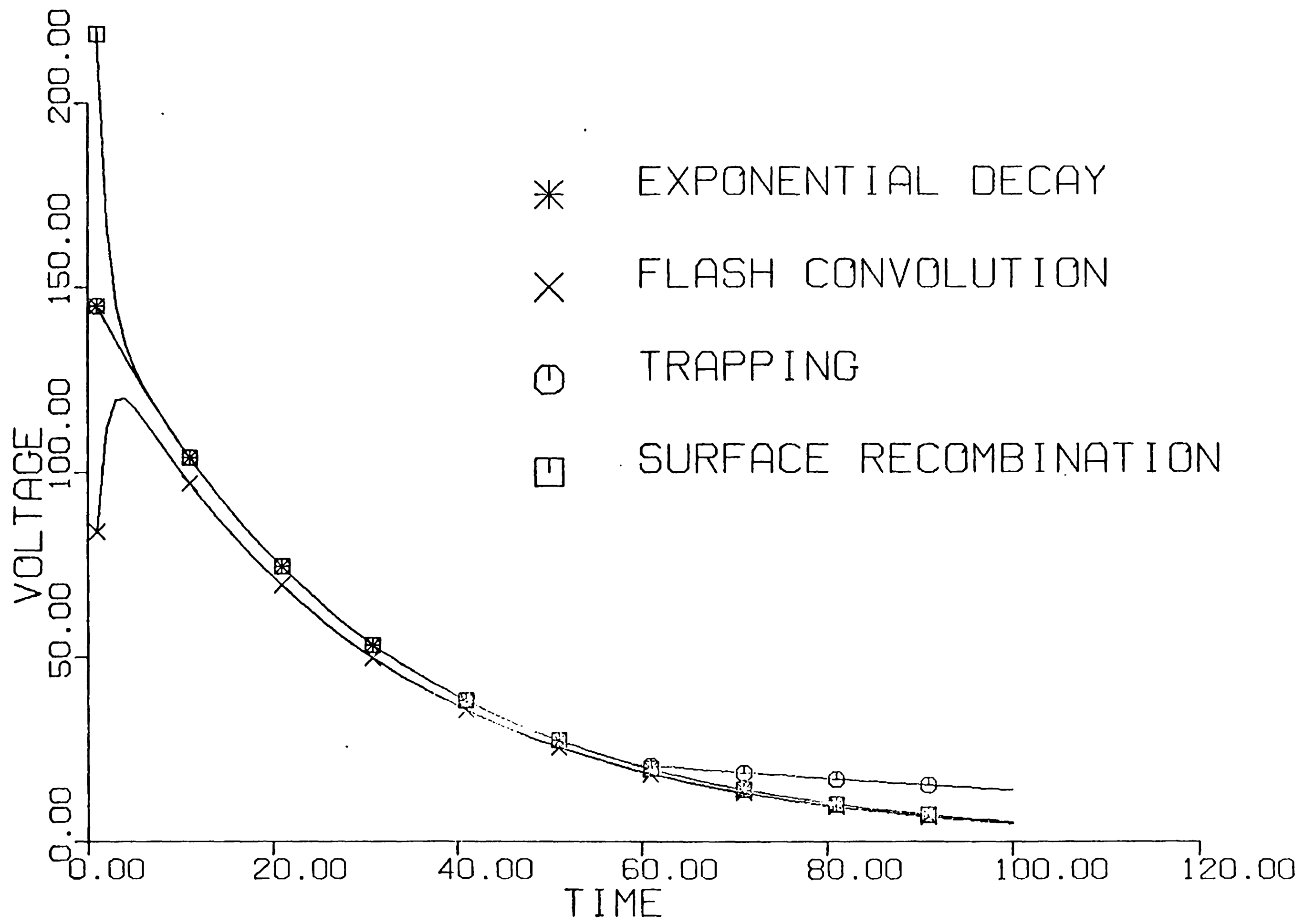

FIGURE 4. EXCESS CARRIER DECAY EFFECTS

VI.RESULTS

As stated in the previous section, three different heat treatment ranges were tried for each type of silicon available. Fast and slow quenches were implemented as described. Also evaluated were gamma irradiated samples of CZ and FZ1. These samples were covered with cadmium foil and irradiated with neutrons in the Virginia Tech reactor. Most of the neutrons were low energy thermal neutrons and were stopped by the cadmium, which then emits a gamma ray. The total gamma ray fluence was estimated to be $5x10^{13}$photons/cm^3. Finally, the impurity grown samples obtained from Westinghouse were also evaluated.

A major experimental difficulty in characterizing recombination centers is reproducibility. Section III indicates the sensitivity to sample purity of recombination center production. This purity dependence can be apparent even in samples cut from the same boule. It was found that samples cut from the boule surface gave poor results in terms of large variations in lifetimes for the same heat treatment. This could be expected since the surface is more vulnerable to rapid temperature fluctuations and impurities. For this reason surface cut samples were not used.

However, it was also found that most of the high temperature (1000-1200C) heat treatments produced lifetimes too small to be of use. Some samples though gave low enough

defect concentrations and their results are given below.

From Table 1 it can be seen that during certain heat treatments both formation and annealing of certain recombination centers can occur. However, it was found that annealing also occurred during measurement in some samples, and for these samples several runs were carried out.

The results are shown in tables 2-7. A slow quench is indicated by slq, and a fast quench by fq. For comparison the graphs for $a\tau_0(1/K_BT)$ have been normalized, and the normalization constant k is given in the tables. The graph and figure number for each sample is also given in the tables, and follow immediately after the table. The heat treatment (HT) time is given in minutes (M) or hours (H). The error in the energy level is given in absolute terms (eV), whereas for clarity under normalization the standard deviation for the curve is given as a percentage. The energy level error is calculated from the point fit to equation IV.17. Additional error contributions due to temperature or voltage errors are not included. Computer simulations show these effects are expected to be small compared to the fitting error. The major uncertainty in the energy level determination is fundamentally controlled by the shift in the gap energy with temperature. Over 50C this can be 0.02eV.(ref.15)

Experience has shown that fits to a seemingly innocuous

form of equation such as III.21 are not straightforward. Convergence depends on the parameters involved and the ranges of the fitted data. Needless to say the requirements of section III must be met. In some sample runs they are not and the Fermi level crosses the recombination center energy. Thus two levels contribute over the temperature range used. This effect is clearly evident in the inverse capture cross section plots, and as a discontinuity in the lifetime measurements. When this occurs a single level fit is clearly nonsense, and where possible, two separate temperature ranges are used, under the constraints of section IV.

Finally, the energy level fit relies on the "A" and "B" parameters (eq. IV.4) being relatively independent of temperature. Their temperature dependence is included in the $a\tau_0$ plot. Thus if this shows a rapid fluctuation with temperature the predicted energy level should be viewed with caution.

Twenty samples obtained from Westinghouse were analyzed. These contained a variety of impurities. Most samples showed too small a lifetime or excess signal or too large trapping to be of use. The results for the usable samples are given in table 7.

Effects from annealing which occurs during a run are catastrophic. Thus the data have to be carefully scrutinized

so as not to include such effects. The data given are those for when no further annealing takes place. If previous annealing has occurred it is noted in the comments column.

The scanning electron microscope micrographs were obtained using the S.E.M. in the college of Veterinary Medicine at Virginia Tech. The samples used were fractured and given a light etch in the chem-polishing acid mixture, in order to highlight any structural defects and regions of stress or impurities. In order to illustrate the effect of the etch which is a redox precipitation reaction, samples were examined unetched. Some FZ 600C fast quenched samples showed signs of cloudiness which may have indicated precipitation, but otherwise the only clear signs of precipitates occur in the FZ 500C fq. The orientation plane of the micrographs is not obtainable due to the high depth of focus of the SEM and the uncertainty in the fracture.

Finally, also included are the results of a resistivity vs temperature plot for a FZ 650C fq and a CZ 375C fq (fig. 5(a),5(b)). The "step" in the plot for the FZ sample occurs when the Fermi level is calculated to be 0.4eV below the conduction band edge, in excellent agreement with the lifetime data. Also the density of the center can be estimated to be about 3% of the equilibrium density or about $10^{12}/cm^3$. The resistivity data were taken using a standard four point probe method.

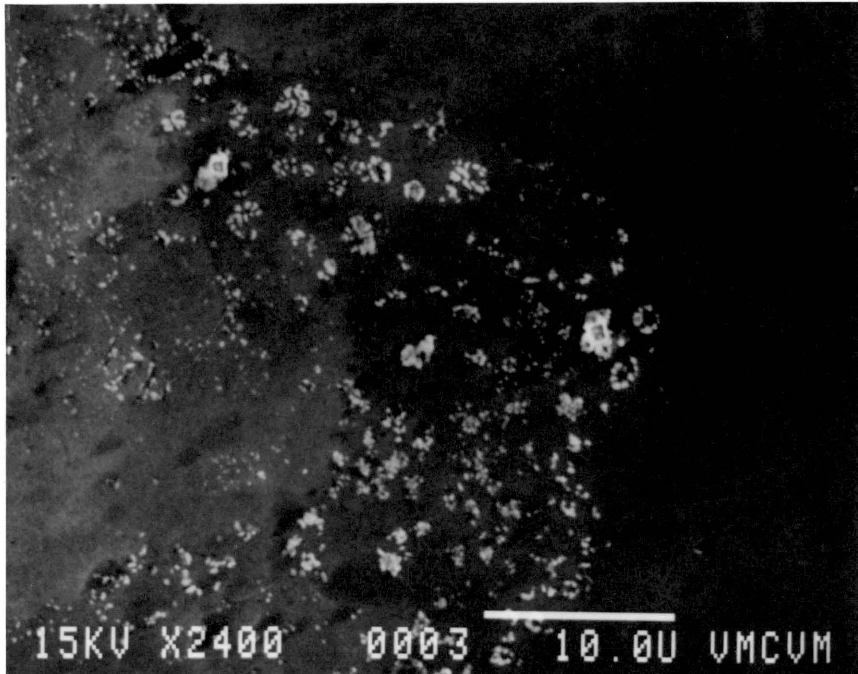

Micrograph (a): Etched FZ sample,untreated.

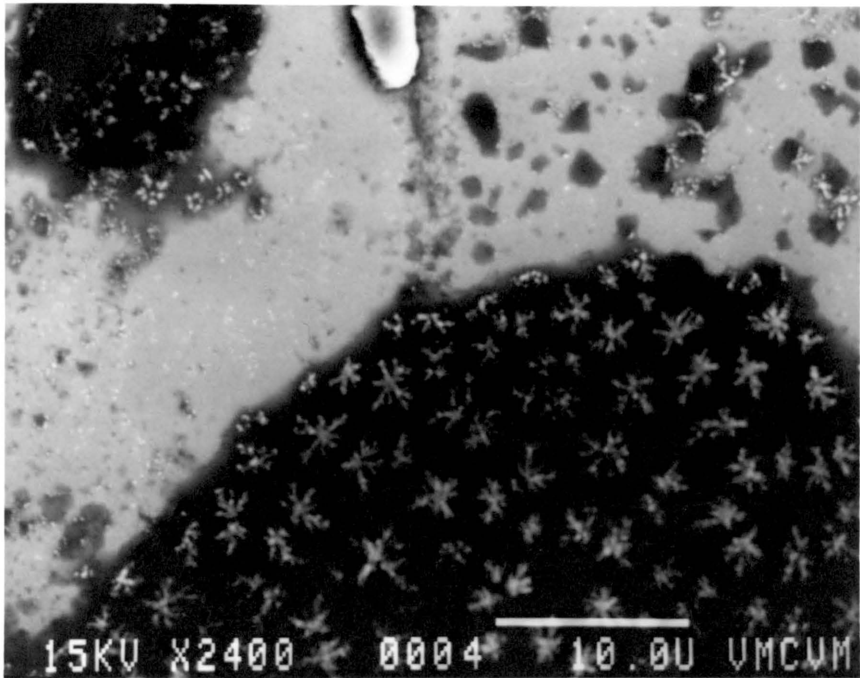

Micrograph (b):Unetched FZ500 C fq.

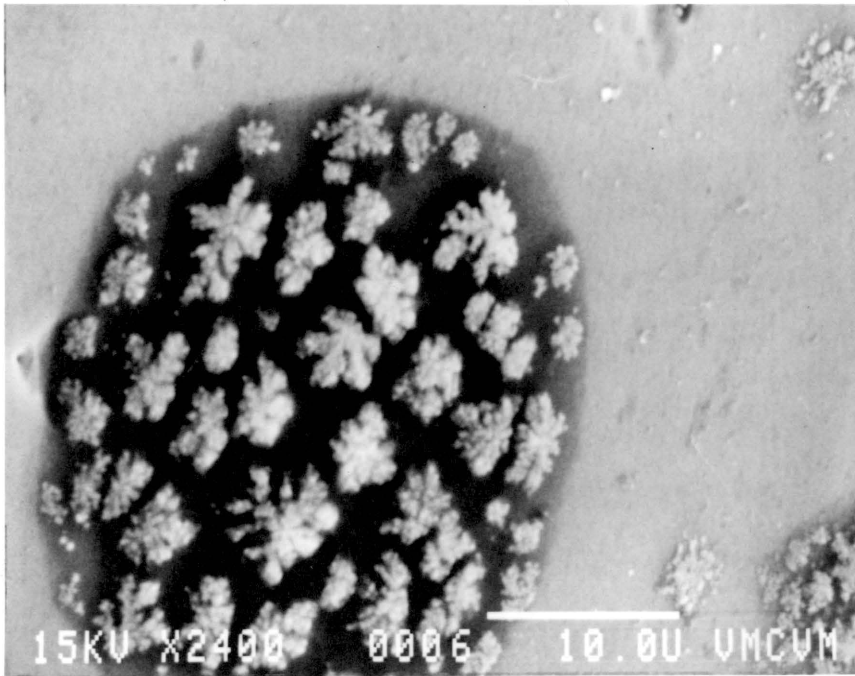

Micrograph (c):Etched FZ500 C fq.

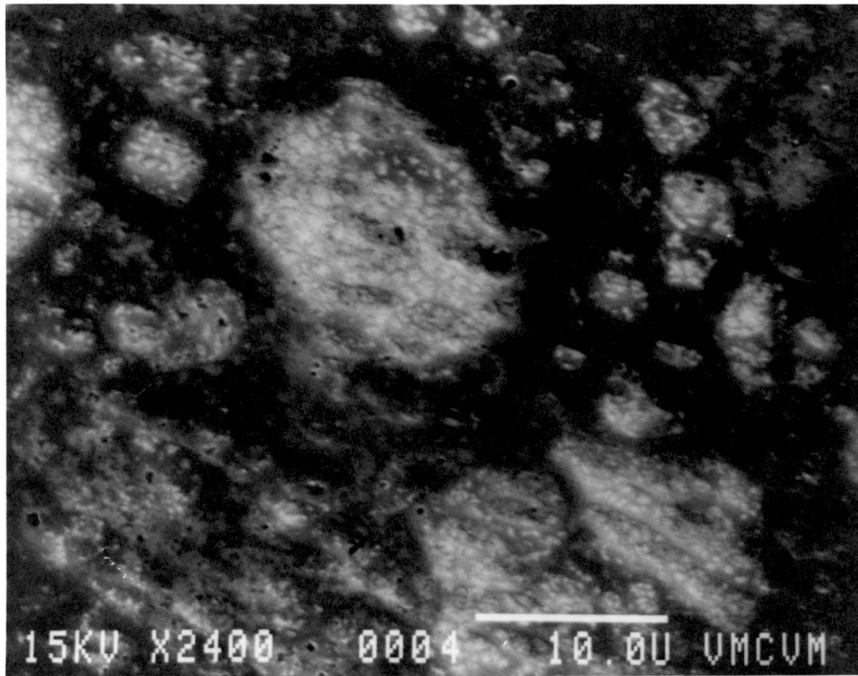

Micrograph (d): Etched FZ500 C slq.

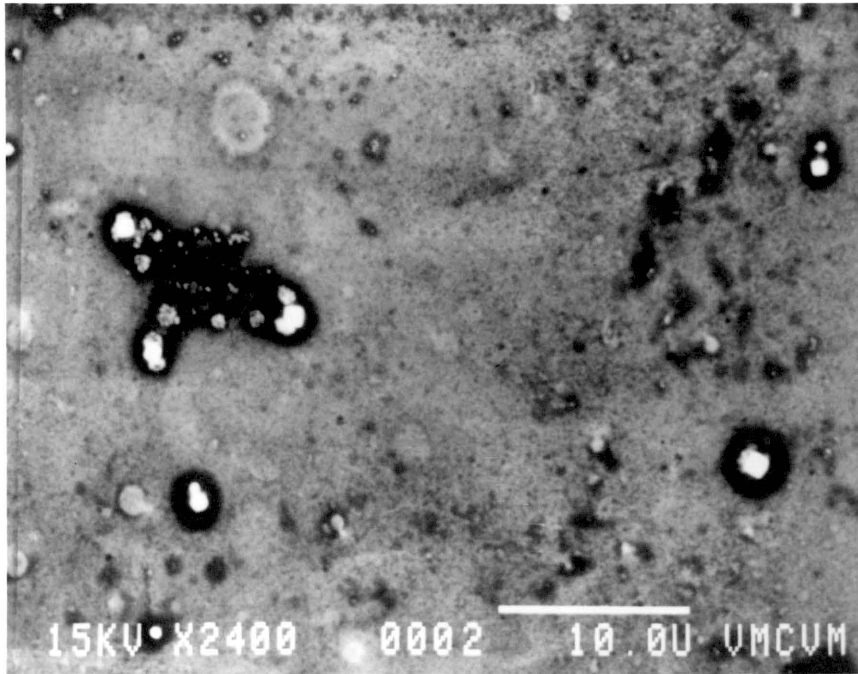

Micrograph (e): Etched FZ650 C fq.

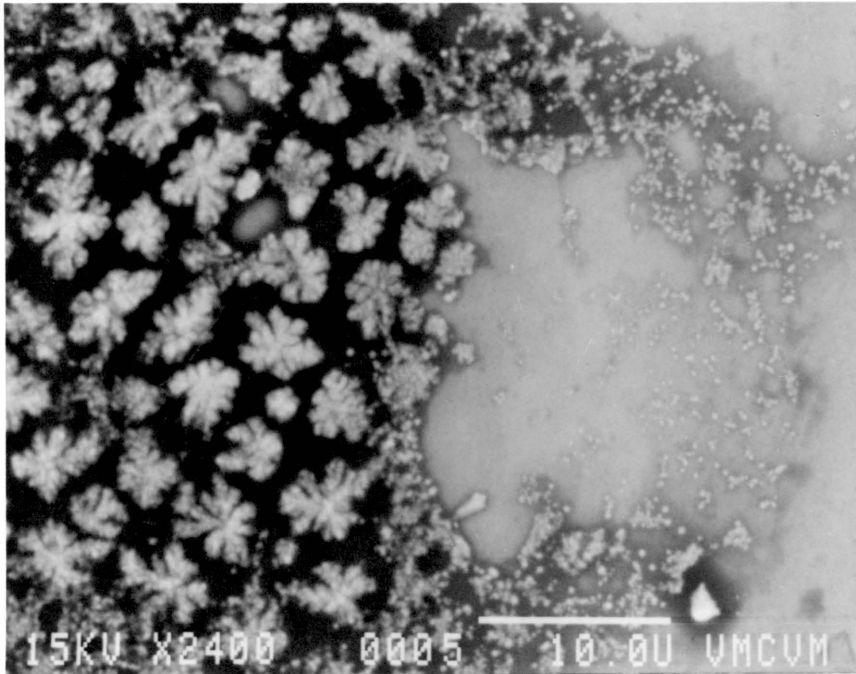

Micrograph (f): Etched FZ65.0 C slq.

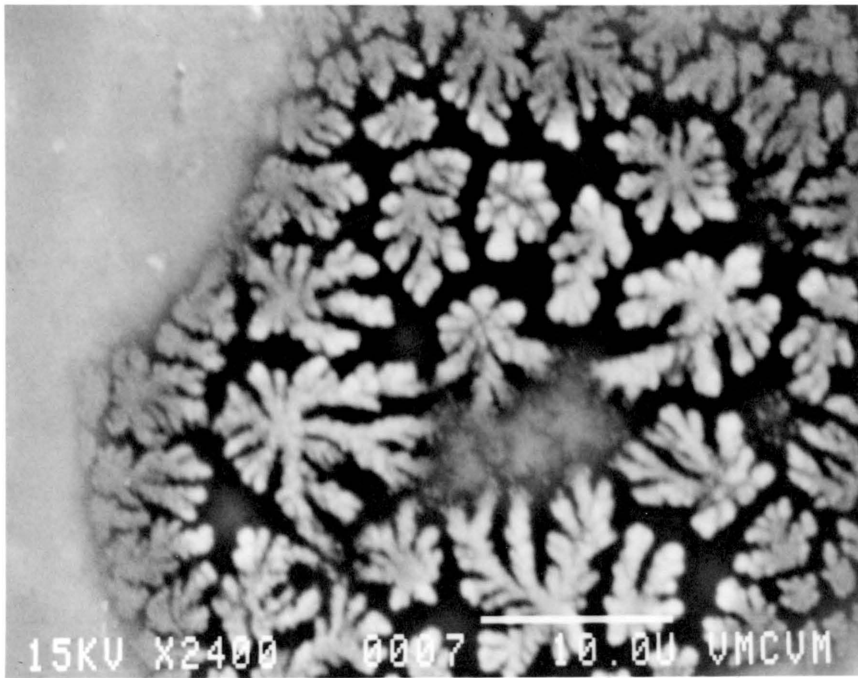

micrograph (g): Etched FZ1000 C fq.

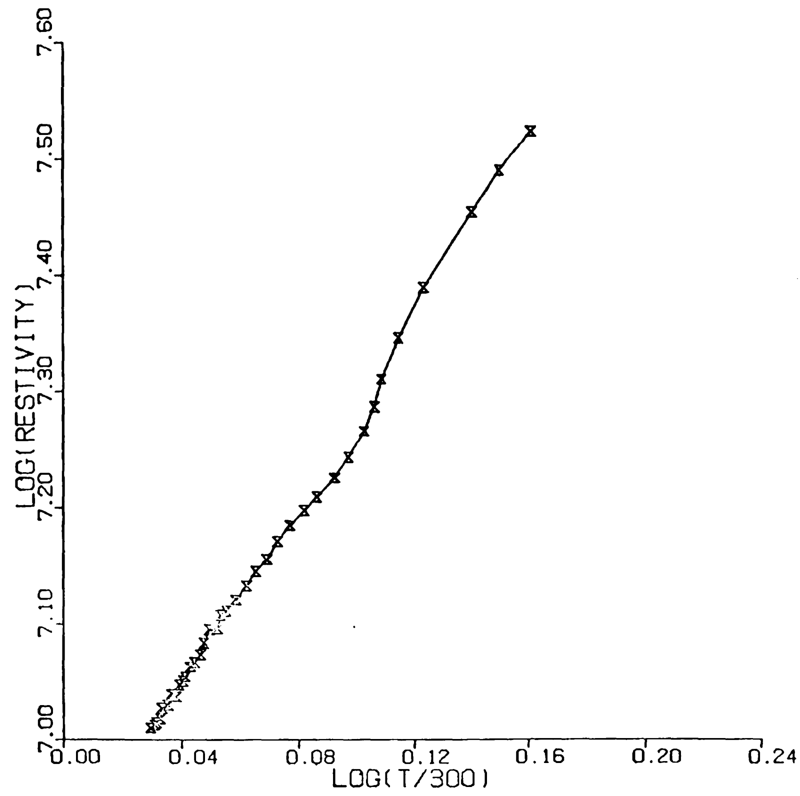

FIGURE 5A. RESISTIVITY ACTIVATION FOR FZ

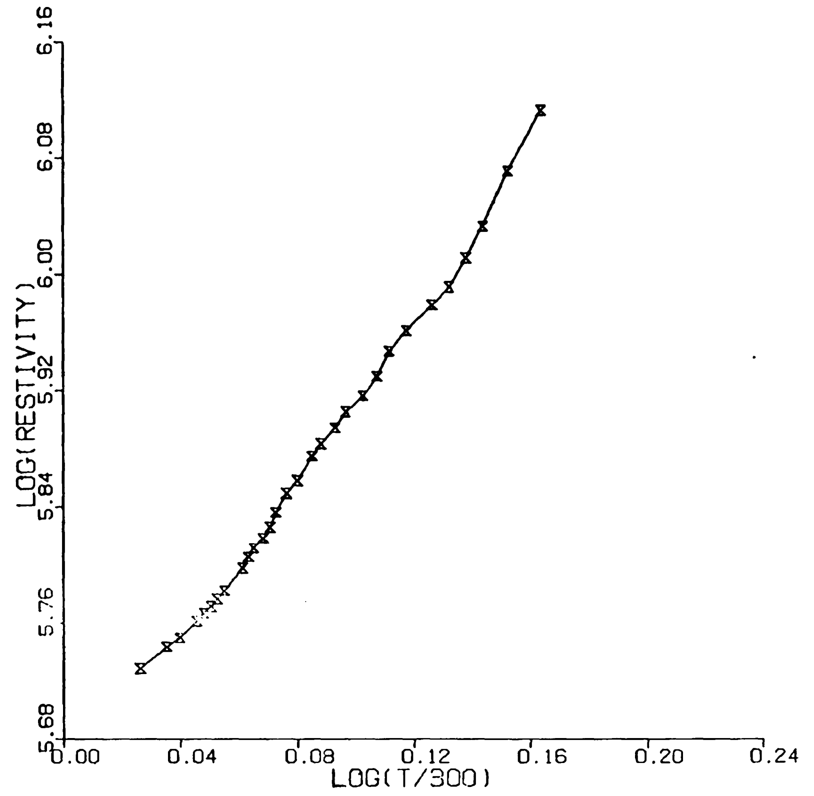

FIGURE 5B. RESISTIVITY ACTIVATION FOR CZ

Table 2.Results for CZ heat treatments

Sample no.	HT time/temp	slq /fq	Energy level(eV)	Fig. for $\tau_{n0}+\tau_{p0}$	k (p.46)	Comment
CZ79	1.25M 650	fq	0.083/0.003	6.3	5.97/4%	note 1
CZA	1.25M 650	fq	0.064/0.001	6.2	40.01/3%	note 1
CZ17	3H 600	slq	0.173/0.003	6.1	2.65/6%	
CZ49	3H 600	slq	0.207/0.007	6.4	3.55/5%	
CZB	1H 375	fq	0.505/0.006	6.5	14.18/3%	

note 1: These samples showed strong annealing during initial runs; also note the large difference in k values, indicating a considerable absolute lifetime difference.

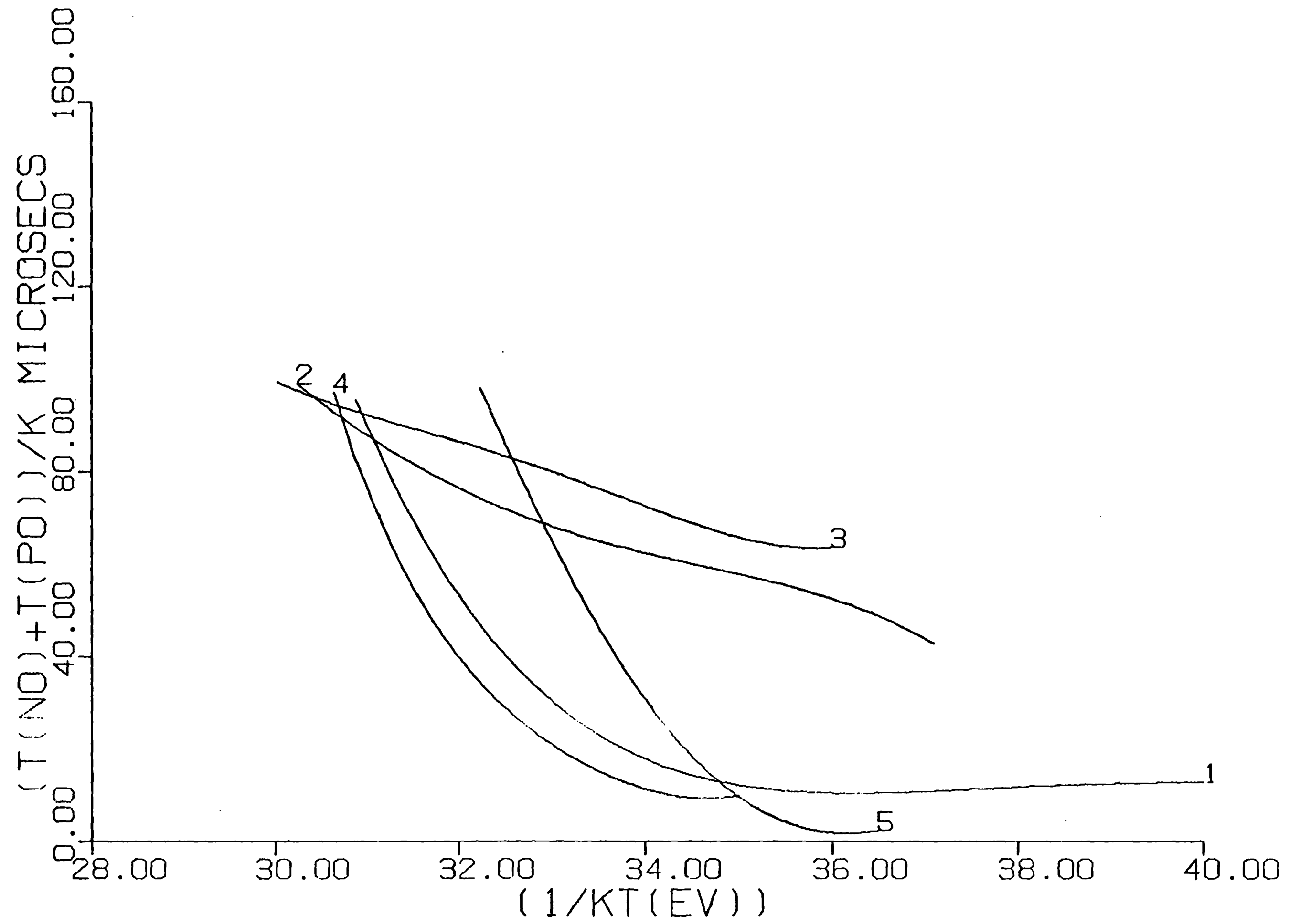

FIGURE 6. FOR CZ HEAT TREATED SAMPLES

Table 3.Results for irradiated samples

Sample no.	HT time/temp	slq /fq	Energy level(eV)	Fig. for $\tau_{n0}+\tau_{p0}$	k (p.46)	Comment
CZA	10H 350		0.125/0.005	7.1	10.24/3%	
FZ1A	15H 170		0.231/0.003	7.4	1.88/2%	
FZ1A	15h 170		0.250/0.004	7.3	3.40/2%	
FZ1B	14H 170		0.280/0.006	7.2	1.53/2%	

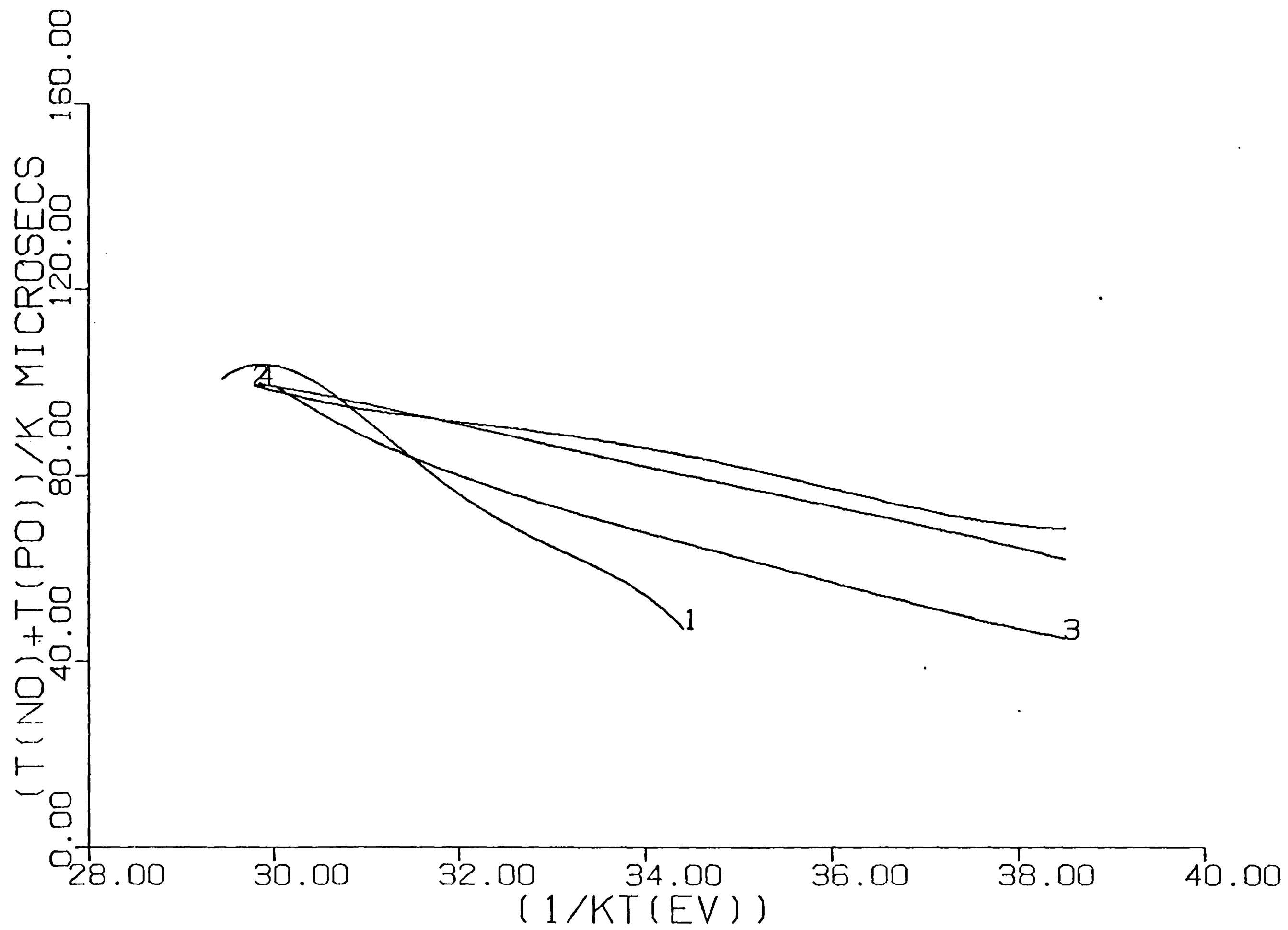

FIGURE 7. FOR IRADDIATED FZ1/CZ SAMPLES

Table 4.Results for FZ1 600/650C fast quenches

Sample no.	HT time/temp	slq /fq	Energy level(eV)	Fig. for $\tau_{n0}+\tau_{p0}$	k (p.46)	Comment
FZ1C	1M 600	fq	0.245/0.008	8.1	0.48/15%	note 1
FZ1B	1M 600	fq	0.187/0.011	8.2	0.78/6%	
FZ1A	1M 600	fq	0.094/0.011	8.3	0.54/15%	note 1
FZ1B	1M 600	fq	0.174/0.012	8.4	0.58/9%	
FZ1D	1M 600	fq	0.182/0.006	8.7	4.68/6%	
FZ1AA	1M 650	fq	0.150/0.007	8.5	2.31/5%	
FZ1BB	1.25M 650	fq	0.097/0.011	8.6	0.57/10%	

note 1: All samples in this table showed strong initial annealing effects, and FZ1A and FZ1C energy levels are considered suspect due to discontinuities in the lifetime measurements which happen to occur at the curve minimum; note also that the raw data seems to indicate that the curve tail does not have a strong slope, so the indicated slope may be due to the fitting routine.

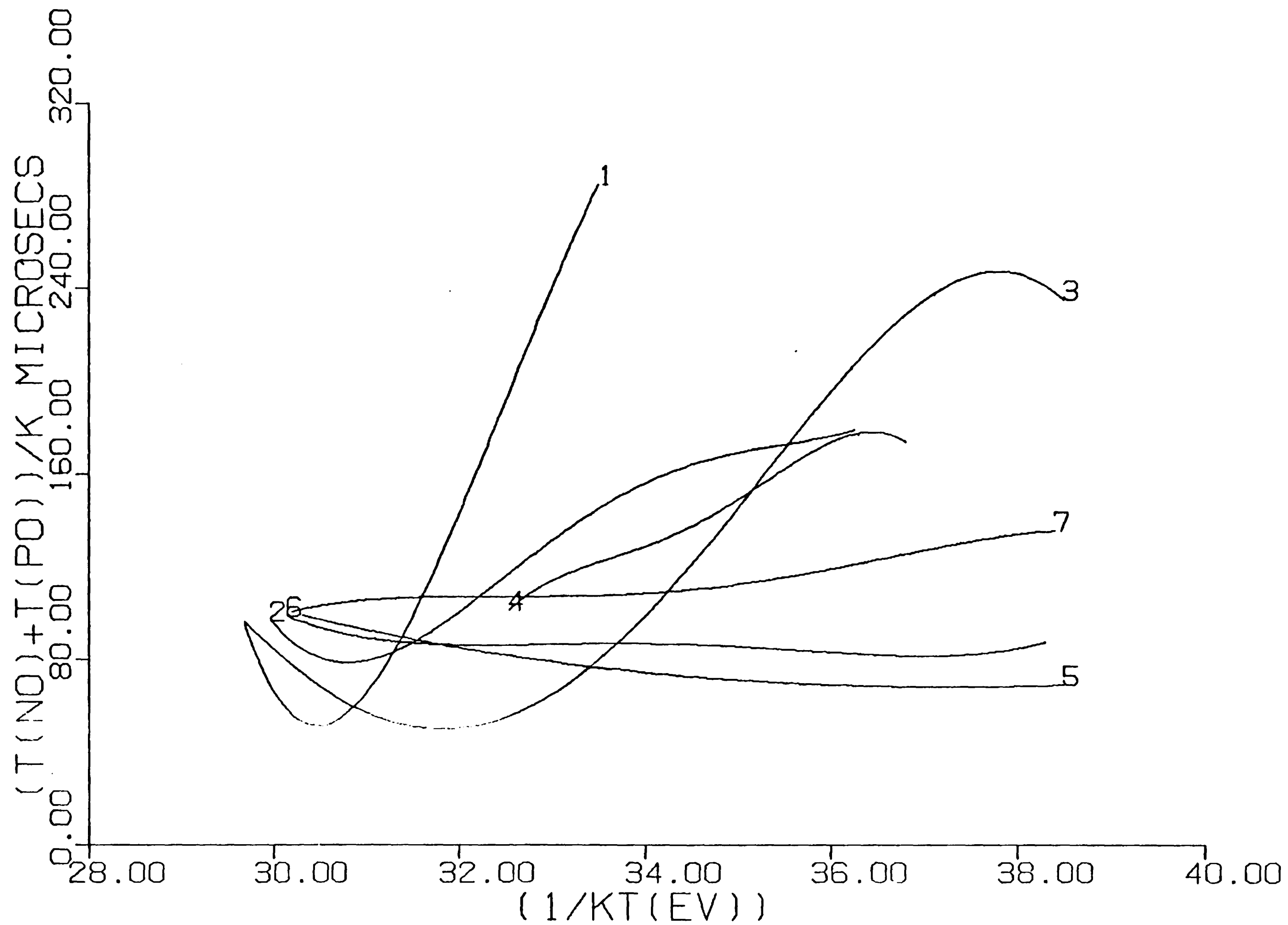

FIGURE 8. FOR FZ1 600/650C FQ SAMPLES

Table 5.Results for FZ1 650C slq and 500C fq heat treatments

Sample no.	HT time/temp	slq /fq	Energy level(eV)	Fig. for $\tau_{n0}+\tau_{p0}$	k (p.46)	Comment
FZ1A	40M 650	slq	0.177/0.004	10.3	16.45/3%	
FZ1B	40M 650	slq	0.195/0.012	10.2	51.94/1%	
FZ1AA	1.5M 500	fq	0.185/0.017	10.1	4.91/5%	
FZ1BB	4.5M 500	fq	0.167/0.035	10.4	0.58/9%	
FZ1C	22H 500	slq	0.248/0.013	9.1	2.21/3%	
FZ1D	14H 500	slq	0.242/0.002	9.2	3.25/2%	
FZ1E	18H 500	slq	0.321/0.008	9.3	12.21/2%	
FZ1F	18H 500	slq	0.283/0.025	9.4	24.04/2%	

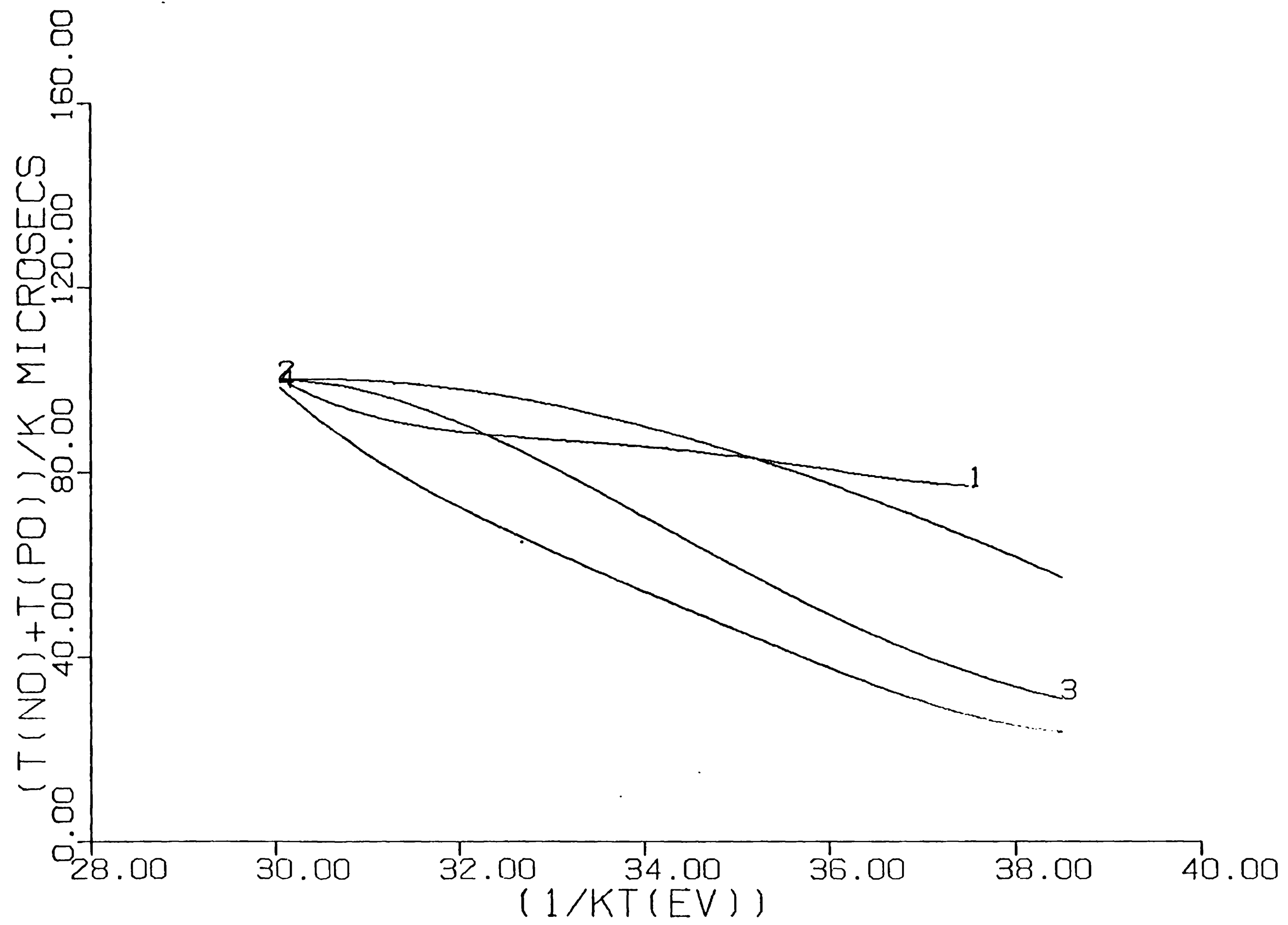

FIGURE 9. FOR FZ1 500C SLQ SAMPLES

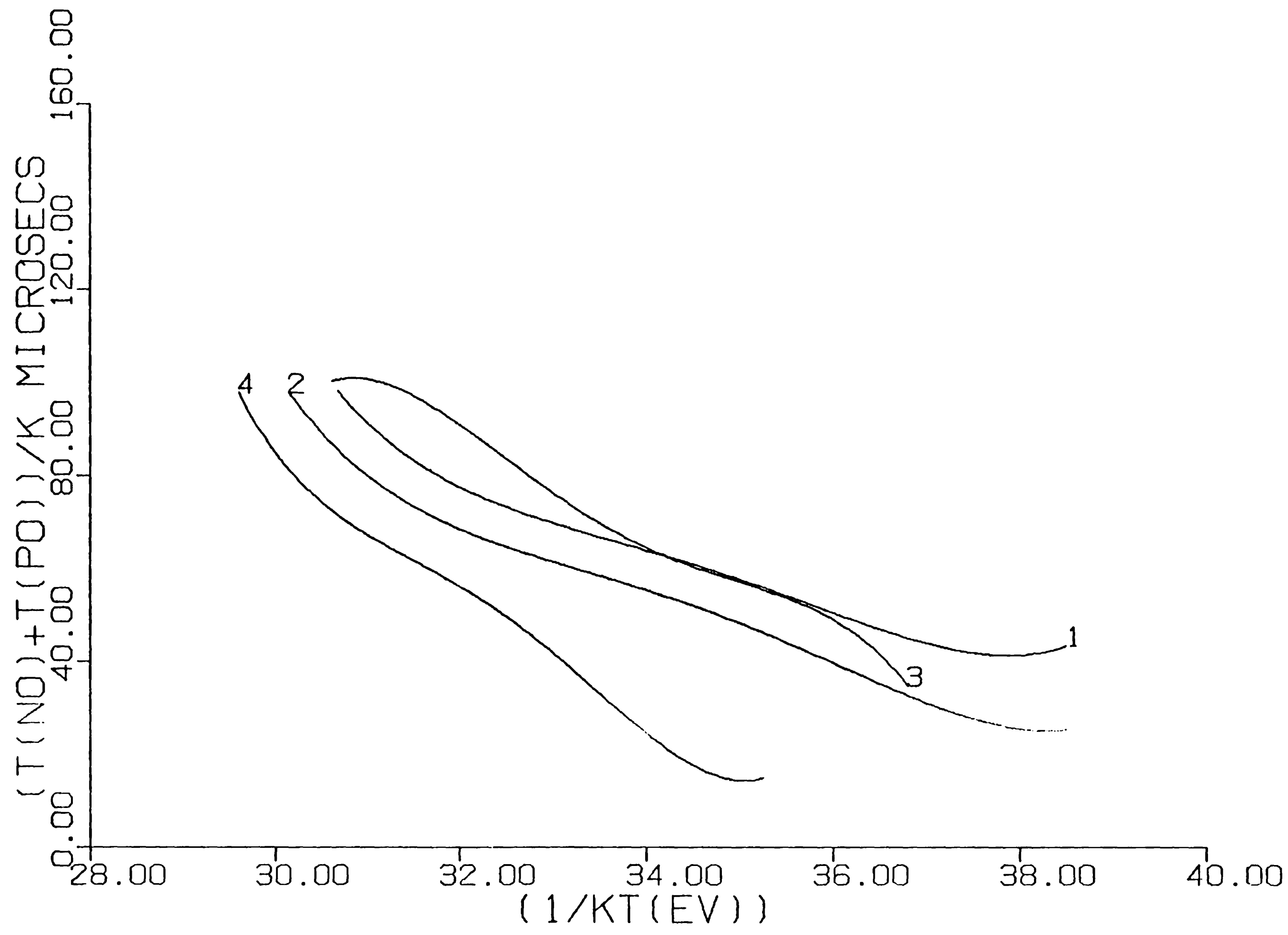

FIGURE 10. FOR FZ1 500C FQ AND 650C SLQ

Table 6. Results for 1000/1260C heat treated samples

Sample no.	HT time/temp	slq /fq	Energy level(eV)	Fig. for $\tau_{n0}+\tau_{p0}$	k (p.46)	Comment
FZ22	6H 1260	fq	0.293/0.007	11.1	0.88/15%	
FZ19	30M 1000	fq	0.256/0.006	11.2	2.75/3%	
FZ5	30M 1260	fq	0.305/0.006	11.3	1.37/2%	

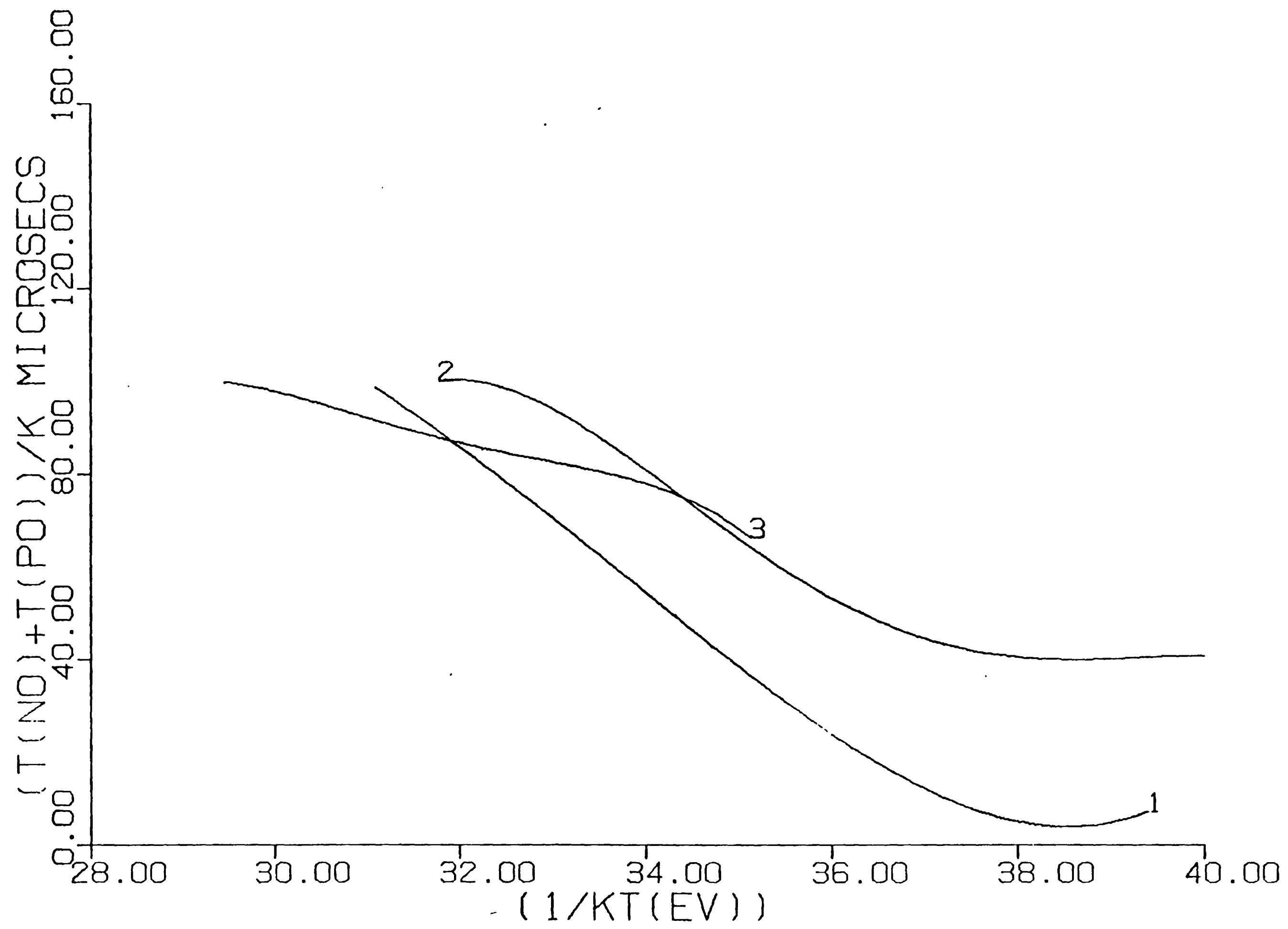

FIGURE 11. FOR 1000/1260C FQ SAMPLES

Table 7.Results for impurity doped samples

Sample no.	HT time/temp	slq /fq	Energy level(eV)	Fig. for $\tau_{n0}+\tau_{p0}$	k (p.46)	Comment
Cu212	As grown		0.253/0.037	12.1/.2	4.74/25%	note 1
Co165	As grown		0.204/0.02	12.3	9.35/2%	note 2
Ni147	As grown		0.28/0.003	12.4	16.35/4%	
Ti232	As grown		0.25/0.02	12.5	2.0/10%	note 3

note 1. The missing section showed no fits for a lifetime determination.

note 2. The variation in the lifetime was approximately 5 microseconds over the measured temperature range, thus the fit should be viewed with caution.

note 3. The temperature range available was not sufficient to obtain a fitted level, so the level is calculated using three points and solving simultaneously for E. The error value is estimated from several such calculations.

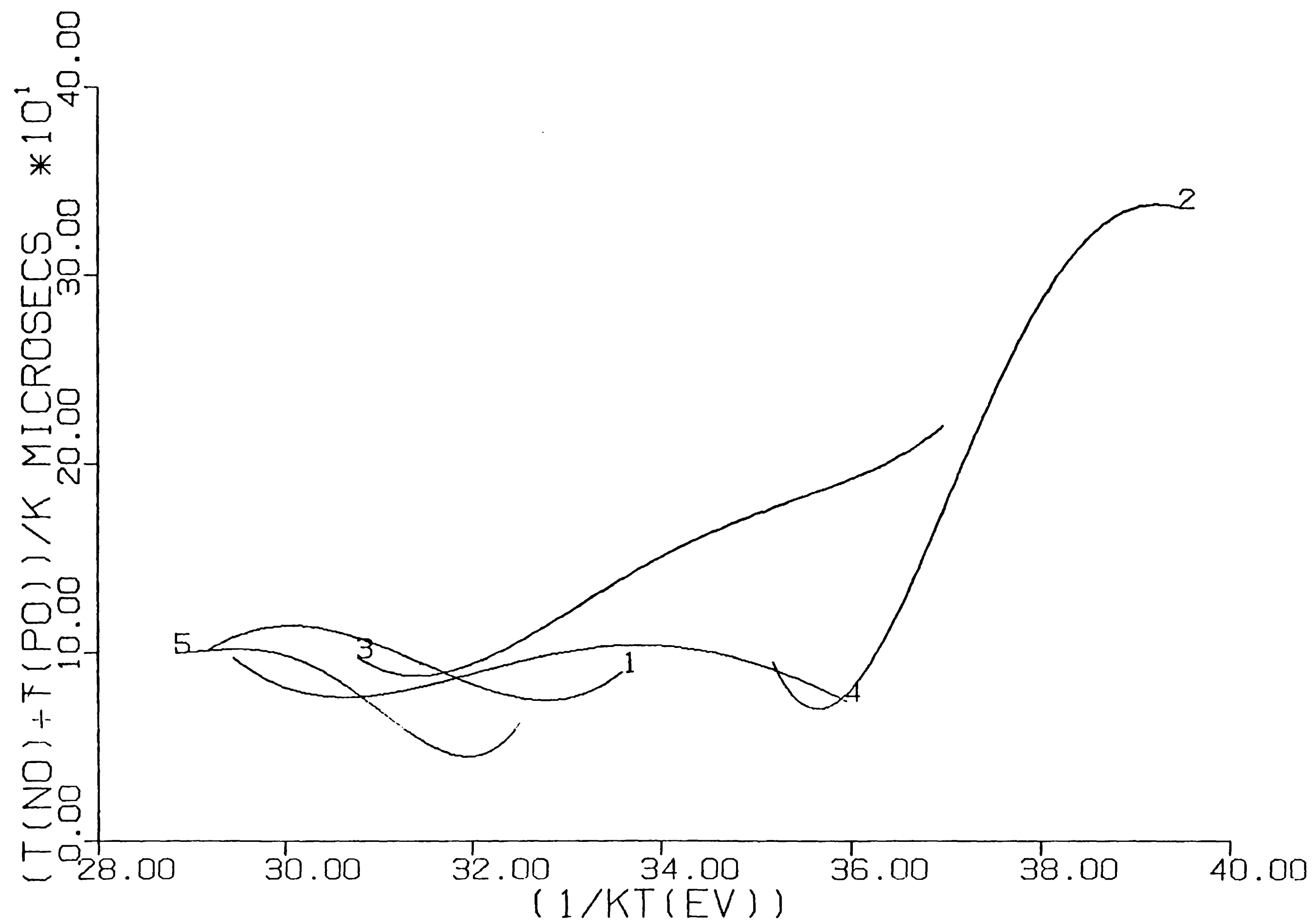

FIGURE 12. FOR IMPURITY DOPED SAMPLES

VII.DISCUSSION

Clearly from the results in the previous section both the lifetime data and the micrographs show a significant variation of defect structure and electrical properties in response to low temperature heat treatments.Since short, low temperature heat treatments have little use in device applications and cannot be studied using standard deep level techniques, little information is available concerning the mechanisms and structure of these defects. However, numerous studies have shown the importance of nucleating centers formed by point precipitates or agglomerations in subsequent high temperature processes, hence the value of this study and the need for a more detailed description of the state of knowledge available.

A fundamental question to ask is: why does a short, low temperature heat treatment precipitate effects not seen when the sample cools down from its molten state, thus undergoing a similar heat treatment (in both cooling rate and experimental conditions)?. Such hysteresis indicates a dependence of the recombination center density on heat treatment direction, i.e. cooling or heating, or a time dependence, say from the initial crystallization. There are also several dynamic processes occurring which depend on heating/cooling rates and absolute temperature, which implies some sort of barrier kinetics. Clearly the ultimate

answer to this question lies in the microscopic interactions of the defects (interstitials, vacancies, impurities) involved.

Before discussing the relevance of this dissertation's results it is necessary to review in greater detail the state of understanding of defects in single crystal silicon and also some of the more widely accepted models of defect structure and dynamics.

i) Vacancies and Interstitials (ref. 17)

a) Relatively low growth rates of 10-15 cm/hr for single crystal silicon boules allows time for the majority of point defects to diffuse out or be annihilated, providing there are no sources available or nucleating agents present to provide a more stable agglomeration mechanism for formation and pinning of such defects (i.e. a non-thermal -equilibrium process).

b) The density of vacancies at melting is estimated to be 10^{13} to $10^{16}/cm^3$.However, due to the high mobility of vacancies and relatively small variation of diffusion coefficient with temperature, quenching of vacancies without some sort of process as described in (a) is not possible.

c) From calculations of formation enthalpies for vacancies and interstitials , approximately 3 eV for vacancies and 8 eV for interstitialcies, it would appear

that the concentration of vacancies should far exceed the concentration of interstitials. However, self diffusion experiments show that several mechanisms are required to explain data over the entire temperature range. At present the contribution of interstitials is necessary to explain self diffusion at high temperatures. The importance of interstitials is also indicated by noting that the majority of crystallographic defects in silicon have been shown to be extrinsicly based (extra impurity atoms or interstitials) rather than vacancy related. One of the major difficulties in determining concentrations of vacancies and interstitials is determining their diffusion coefficients or migration enthalpies. The calculation of these values is highly dependent on temperature range and experimental procedure.

d) A fairly recent proposal to explain these observations is that a self interstitial occurs in different charge states and configurations which are dependent on temperature. Each charge state(I^+, I^o, I^-) has a different mobility, formation enthalpy and energy level. The basic effect postulated is that as the temperature rises the electronic state of the interstitial becomes more extended. Thus in order to migrate the defect has to break more bonds, and from this it is deduced that as the temperature increases the enthalpies of formation and migration also increase according to the state. Experimental evidence

seems to indicate the annealing temperature ranges of these defects as 140-170K, 370-420K and 540-600K. Clearly the charge state also depends on the position of the Fermi level, so the configuration of the interstitialcy depends on the carrier concentration and doping level.

ii) Microdefects (ref. 17)

a) The two major types of microdefects have been described in section III. "A" defects are small dislocation loops approximately 3-5 micrometers in diameter and "B" defects are probably small interstitial clusters one tenth this size.

b) In as grown single crystal silicon the concentration of "A" defects is of the order of $10^6/cm^3$ and "B" defects 10^7-$10^{11}/cm^3$. The formation of these defects is suppressed in the presence of dislocations and also no "A" defects appear near the surface of the boule. "A" defects are thought to form at lower temperatures than "B" defects and are considered to be a product of "B" defect condensation.

c) The interstitial nature of these microdefects implies that their formation requires extra atoms, either interstitials or impurities, to provide a compression stress to generate further interstitials. There is evidence which shows that the identity and size of microdefects is linked to oxygen and carbon concentrations, and the nuclei for microdefect formations are thought to be caused by

oxygen/carbon impurity striations generated by temperature fluctuations during crystal growth. (refs. 13,16)

iii) Impurities (refs. 13, 16)

a) The major impurity processes have been described in section III, but it is worthwhile to note the following facts. As-grown silicon should become supersaturated with oxygen and carbon around 800 to 1000C. At these temperatures the diffusion length for oxygen in one second is only 2 to 3 nm.

b) In supersaturation interstitial oxygen readily forms complexes with silicon (especially in the presence of vacancies), provided some sort of growth barrier is overcome. It is postulated that these silicon-oxygen complexes have a compression field which leads to interstitials and large scale dislocation growth. (refs. 8,13)

c) The initial growth/nucleation process is the mechanism least understood. At present the initial nucleus for the complex is thought to be provided by either point vacancies or interstitials or carbon atoms or some agglomeration of these.

d) The complexing of other impurities such as the metallic impurities used in this study are not understood at the point defect level, though large scale precipitation effects at dislocations have been observed. Their affect on

recombination lifetime has been inferred from device efficiencies of solar cells and can be observed directly.

The following discussion is intended to point out agreements between the results obtained using the lifetime parametrization technique used in this study and other techniques such as EPR or resistivity activation. (table 1, refs.11,17) It will be seen that the energy level results agree fairly well with other techniques, and the temperature variation of capture cross sections as well as the micrographs are not incompatible.

Due to the complexity of reactions possible during the fracture and etch processes any connection between the micrographs and the electrical data is clearly circumstantial and tenuous. However, comparisons of micrographs of samples given different heat treatments seem to show precipitation differences even in the unetched samples. This would suggest the precipitates are real and not simply due to the decoration etch. The star-like precipitates and the cloudy regions seen in the unetched sample (micrograph b) have been reported previously (ref.3). They are thought to be some type of oxygen precipitation.

Conversations with material scientists support this identification, but no techniques are available either to identify the precipitates positively or to connect them with

the electrical properties observed.

The micrographs show typical examples of the observed precipitates and region size (where applicable). These regions are not extensive over the sample and are scattered randomly over the surface examined. They have an average repetition length of the order of several hundred microns. The FZ 500C (figures 9.1-4 for slq, 10.1, 10.4 for fq) heat treatments clearly show electrical and structural differences between the fast and slow quenches used. Again the regions roughly circular in shape and size are fairly typical of a limited number which are randomly distributed every few hundred microns.

It is very inviting to connect the fairly large variation in energy levels for the slow quenched samples (table 5) with the lack of precipitation, (micrograph d) and the more structured defects of the fast quenched samples (micrographs b, c) to their more precise energy levels (table 5). However, the connection between these precipitates and the recombination centers is only circumstantial, although no other differences were observed at these magnifications (further magnification greatly degrades the resolution). The FZ 500C slow quench energy levels are compatible with the levels for the silicon divacancy complex and the 500C fast quench with the A center (table 1). The FZ 650C slow quenched samples and the FZ

500C fast quenched samples show agreement in levels (table 5) and plots (figure 10.1-4) and seem to be compatible with the A center. Both also show similar precipitation in the etched samples (micrographs b, c, f) although no precipitation was observed in the unetched FZ 650C samples.

the lifetime annealing seen in the 650C fast quenched FZ samples (table 4 notes) would seem compatible with the lack of formation of precipitates. Intuitively it seems more feasible for small defects to be either more mobile than larger ones and thus sensitive to annealing, or for them to create stress fields or impurity gradients which assist some annealing processes of smaller defects. The energy level analysis supports the connection between the precipitates and the recombination defects, all 650C slow quench (table 5) and 500C fast quench samples (table 5) having similar values. Table 1 would indicate this center to be a vacancy/oxygen complex. The CZ 600C slow quench also has the same level but a different and larger temperature dependence (table 2). Since a strong temperature dependence can affect the energy level fit (eq.IV.4), the predicted level should be viewed with caution.

The 650/600C fast quench energy levels (table 4) are more complex to analyze but contain more information. The CZ 650C fast quench samples (table 2) both show the dominant recombination level to be shallow with considerable

annealing taking place, possibly indicating another less stable level present. Although the donor complex at E_c-0.08eV is supposed to be unstable at 650C, a quench from this temperature might be expected to show some annealing of this level. the annealing can clearly be seen as a lifetime change during a run and on successive runs. (table 4 notes)

the FZ 650/600C fast quenches (table 4) are certainly the most complex and show the most sample dependence. Even after all annealing has occurred it is obvious from the variation in the capture cross sections with temperature that a complex mechanism is still ocurring (figures 8.1-7). The data are compatible with the existence of two recombination centers, at least one of which is Fermi level dependent and undergoes a certain degree of annealing.

The evidence for such centers is twofold. First, while annealing the lifetime data indicates a deeper level (greater than 0.33 eV) responsible for recombination while the Fermi level is deeper than 0.4 eV (approximately), then as the temperature decreases another shallower and more stable level takes over. An interesting additional fact, which tends to support this view is that the lifetime decreases with annealing in these samples, whereas in other samples annealing increases lifetime and so indicates a diminishing number or consolidation of recombination centers. Secondly, the position of the minimum in the

capture cross section curves (figures 8.1, 8.3) indicates a change in behaviour when the Fermi level is in a similar position (calculated from temperature and carrier concentration). The evidence thus points strongly to a two-level system being responsible for recombination in the FZ 600/650C fq samples, with at least the deeper level being Fermi level dependent.

The lifetimes and calculated energy levels for the irradiated samples clearly show a dependence on the oxygen content of the silicon used (table 3). The fact that only one out of four CZ samples irradiated gave a result also illustrates the differing reactions of the CZ and FZ types. The range of energy levels obtained for the FZ and the fact that significant annealing is necessary to obtain a measurable lifetime, indicates a dynamic process which may not be in equilibrium.

The impurity doped samples gave mixed results (table 7). Copper has a reported donor level from EPR studies at E_v+0.24eV (ref.18) which is compatible with the discontinuity in the lifetime data (table 7 note 1). The temperature ranges giving data outside this region are too small to obtain accurate energy level data (figures 12.1, 12.2). The fitted levels are compatible with a two-level recombination system and the capture cross section curves support this assignment (figure 8).

the nickel doped sample (table 7) showed a level at 0.28eV which is in exact agreement with a reported acceptor level at E_c-0.28eV (ref. 18). Also another nickel doped sample having a Fermi level in approximately this energy range displayed resistivity behaviour compatible with this level. The titanium sample (table 7) as stated in the results section shows behaviour which can be explained using a two-level contribution, the high temperature level being tentatively compatible with the reported level at E_c-0.26eV.(ref.18) The result for the cobalt doped sample (table 7) does not agree with any level reported in the literature and (table 7 note 3), due to the small change in the lifetime, the data fit and level should be viewed with caution.

Ideally one would like to compare the experimental curves obtained for $\tau_{n0}+\tau_{p0}$ with the theoretical predictions for capture cross sections from section III, $\tau=1/(N\sigma v_{th})$. However, since the temperature dependences are so model/parameter dependent, it seems impossible to make anything further than a generalized comparison.

If one takes into account a $T^{0.5}$ contribution from the thermal velocity term, most of the experimental data is compatible with the small negative power dependences predicted for the attractive or neutral centers in the cascade model. The copper impurity sample shows a

relatively temperature independent portion followed by a rapid growth (figures 12.1, 12.2), and this agrees with the predicted donor level at E_V+0.24eV, the rapid growth occurring while the charged state of the donor acts as a recombination center.

As stated before the temperature behaviour of the FZ 650/600 fast quench samples shows (figures 8.1-7) the greatest variation. Samples FZ1B and FZ1D received the same heat treatment and both show an increase on the plot for a similar energy level. However, from the k column (table 4) the absolute magnitudes of the plots vary considerably (approximately a factor of 7). This indicates that the number of centers created is strongly sample dependent. FZ1AA and FZ1BB both received a 650C fq, but FZ1AA shows an energy level and temperature dependence very close to similarly treated CZ samples (table 2). Probably the clearest deduction to be made concerning this set of data is that the lifetime and other results depend on the choice of sample.

To summarize; semiconductor grade silicon has the reputation of being one of the purest commercially used materials available, effectively dislocation and impurity free. To an extent this is true; however, when viewed in terms of the defect densities analyzed in this study(1:10^{10}), silicon contains impurity densities many

orders of magnitude greater than desired. From this viewpoint it is not suprising to see a large sample dependence and complexity of defect reactions and to find that even after thirty years of study the state of understanding of such matters leaves a lot to be desired. Reproducibility has always been poor, and cross correlation between experimental methods has been limited by the narrow ranges of application for each technique.

As a characterization technique the method developed and used in this study shows promise. Similar sample heat treatments show excellent agreement in temperature dependences and energy levels even for a large variation in defect density(see the k column in the tables). Unlike with many other techniques such as EPR and DLTS, the present method allows a much larger range of possibilities in the choice of sample and its preparation. Also the measurements can be made around room temperature and require a smaller temperature sweep. However, as a technique for determining fundamental physical properties and processes there is some real difficulty in the lack of agreement between theoretical models and between theory and experimental results. Until a satisfactory model encompasses all important aspects of deep levels (potentials, lattice coupling/distortion, etc), the situation is likely to remain confused.

The experimental arrangement used in this study is only

considered as a proof of principle, and it has great potential for improvement. The primary improvement would be using a shorter, stronger light pulse. The strict spectral requirements for this pulse impose limitations on the present apparatus, but additions such as tunable laser diodes or LED banks could be expected to provide order of magnitude improvements. Other refinements such as greater computing power and faster electronics would also help to make this technique a more powerful tool.

Conclusion

A new method has been developed for parametrizing deep levels in silicon. The technique analyzes recombination lifetime decay curves using the Hall-Shockley-Read model for minority and majority carrier lifetimes.

The levels responsible for recombination were determined in samples of semiconductor grade silicon which had undergone controlled heat treatments or gamma irradiation as well as samples containing grown-in impurities.

The sensitivity of the recombination lifetime measurements enabled these levels to be determined in extremely low densities and under bulk conditions which preclude observation by other techniques. In most cases the agreement between the predicted and measured values was good, and the technique possesses good potential for further development.

REFERENCES

1) "Recombination Mechanisms", V.L. Bonch-Bruevich, E.G. Landsberg, Phys. Stat. Sol., 29, 9, 1968.

2) "Radiation damage in neutron transmutation doped silicon: Electrical properties study", R.T. Young, J.Appl.Phys., 49(9), Sept. 1978

3) "Diffusion Mechanisms and Point Defects in Silicon and Germanium", A. Seeger, K.P. Chik, Phys. Stat. Sol., 29, 455, (1968).

4) "Techniques for Obtaining Recombination Center Parameters from Carrier Lifetime Studies", J.R. Srour, O.L.Curtis, J. Appl. Phys., p. 1779, vol.43, No.4, April 1972.

5) "Transient Recombination of Excess Carriers in Semiconductors", G.K. Wertheim, Phys. Rev., p. 1086, vol.109, No.4, feb.1958.

6) "The electronic structure of impurities and other point defects in semiconductors", S.T.Pantelides, Reviews of modern Physics, p. 797, vol.50, No.4, Oct.1978.

7) "Lattice Relaxation and Multiphonon Transitions", K.Huang, Contemp. Phys., p. 599, vol.22, No.6, 1981.

8) "The effects of heat treatments on dislocation-free oxygen-containing silicon crystals", P.Capper, A.W. Jones, E.J. Wallhouse, J.G. Wilkes, J.of Appl.Phys., p. 1646, vol.48, No.4, April 1977.

9) "IRE Standards on Solid State Devices: Measurement of Minority Carrier Lifetimes in Germanium and Silicon by the Method of Photoconductive Decay", Proceedings of the IRE. p. 1292, vol.49, August 1981.

10) "Experiments on the origin of process-induced recombination centers in silicon", C.T.Sah, C.T.Wang, J.of Appl.Phys., p. 1767, vol.46, No.4, April 1975.

11) "Recombination at Deep Traps", H.J. Queisser, Solid State Elec., p. 1495, vol.21, 1978.

12) "Radiation Damage in Lithium Counterdoped n/p Silicon Solar cells", A.M. Hermann, H.J. Queisser, Solid State Elec., vol.22, 1978.

13) "Impurities and Imperfections in Semiconductor Silicon", Ravi, New York press, Wiley, 1981, chap. 3.

14) "Experimentation: An Introduction To Measurement Theory and Experimental Design.", D.C. Baird, Prentice Hall inc., New Jersey, chap. 12.

15) CRC handbook of Chemistry and Physics. 56th Edition, Editor-in-chief R.C. Weast, CRC press.

16) "Advances in Silicon Technology for the Semiconductor Industry. Part II " R.B. Swaroop, Solid State Technology, July, 1983.

17) "Low Temperature Dependences of Nonradiative Multiphonon Carrier Cross Sections of Deep Traps in Semiconductors.", R.Passler, Phys. Stat. Sol. (b) 83, K111

1977.

18) "Deep levels in semiconductors.", M.Jaros, Advances in Physics. 1980 Vol. 29, No. 3, 409 525.

The vita has been removed from the scanned document

RECOMBINATION LIFETIME ANALYSIS

OF DEEP LEVELS IN SILICON.

by

Murray John Robinson

Committee Chairman: T.E.Gilmer Jr.

Physics

(ABSTRACT)

By the addition of selected impurities to silicon it is possible to affect its physical, optical and electrical properties to a remarkable extent.

Of great technological importance are the elements of groups III and V which introduce shallow acceptor and donor levels and control the equilibrium charge density. These levels have been studied extensively and are well understood.

However, other impurities and structural defects are known to introduce deep levels. These levels may act as acceptors or donors in the traditional sense but they can also control the recombination of non-equilibrium charge carriers.

The properties of these recombination levels reflect the processes of energy exchange and provide information on

the defect structure and energy spectrum and are thus of physical interest. Also since they control the excess carrier lifetime which is a critical parameter in many semiconductor devices they are of interest to the technologist.

The major difficulty in analyzing these levels arises from the catalytic nature of the recombination centers which allows an extremely low density of centers to significantly affect the recombination lifetime.

Most bulk single crystal silicon techniques applied to date use activation processes with high resistivity, high recombination center density samples. This severely limits the range and sensitivity of analysis.

In this dissertation is detailed a new approach to more accurately determine lifetime parameters in conjunction with a phenomenological model which describes the recombination using a set of characterizing parameters. The technique is used to characterize the levels responsible for recombination in single crystal silicon after controlled heat treatments and, also, in gamma irradiated and impurity containing silicon.